Faculdade de Engenharia da Universidade do Porto/
Instituto de Ciências Biomédicas Abel Salazar

Development of an anti-adhesive coating using an extracellular polymer produced by a cyanobacterium: towards industrial application

Jorge Alexandre Ferreira Matinha Cardoso

Master Degree Dissertation
Integrated Masters in Bioengineering
(Molecular Biotechnology)

Supervisor: Rita Mota (Junior Researcher)
Co-supervisor: Fabíola Moutinho (Junior Researcher)

September/October 2018

"Tell me and I forget, teach me and I may remember, involve me and I learn."

Benjamin Franklin

Acknowledgements

This work was financed by FEDER - Fundo Europeu de Desenvolvimento Regional funds through the COMPETE 2020 - Operacional Programme for Competitiveness and Internationalisation (POCI), Portugal 2020, and by Portuguese funds through FCT - Fundação para a Ciência e a Tecnologia/Ministério da Ciência, Tecnologia e Ensino Superior in the framework of the project "Institute for Research and Innovation in Health Sciences" (POCI-01-0145-FEDER-007274), by the project NORTE-01-0145- FEDER-000012, Structured Programme on Bioengineering Therapies for Infectious Diseases and Tissue Regeneration, supported by Norte Portugal Regional Operational Programme (NORTE 2020), under the PORTUGAL 2020 Partnership Agreement, through the European Regional Development Fund (ERDF), POCI-01-0145-FEDER-028779 and the AntiBioCoat project (Anti-adhesive Biopolymer Coating) - RESOLVE 2016: Technology Transfer Ignition Program in the Health Sector, Portugal (NORTE2020) (NORTE-01-0246- FEDER-000018-RESOLVE-55536).

I would like to thank all of the people that helped me and support me during this journey.

Firstly, I would like to give my huge appreciation to all the patience, consideration and understanding of my supervisors, that have been incredibly helpful and have involved me with great knowledge. With no doubt that I had the best supervisors that I could ever desire.

I also give a special recognition to all the member of the groups within I was included (Bioengineered Surfaces and Bioengineering and Synthetic Microbiology), that have welcomed me so nicely, particularly, to the group leaders Cristina Martins and Paula Tamagnini.

I would also like to kindly thank Bruna Costa, who have shared with me all the knowledge and experiences developed during the current work, for all the help, kindness and friendship.

A special thanks To CeNTI (Centre of Nanotechnology and Smart Materials) and the personnel and technicians (particularly to Ana Cardoso, Lorena Coelho and Nuno Azoia) who have tremendously contributed for the development of this work. I take in consideration all the cooperation and support, not only with materials and equipment's but also with their goodwill and sympathy.

Also to Daniela and Eng. Carlos Sá from CEMUP (Centro de Matereais da Universidade do Porto), who have generously helped with all of SEM and XPS analysis procedures.

To i3s, and the technicians who were always available to provide me the best integration and help during all the work development.

I would also like to thank Necton company for kindly supplying the NutriBloom Plus commercial media.

Last but not least, a huge gratitude to all my family and friends, who have supported and comforted me at the good and not so good moments, always giving me the inspiration and avidity for the accomplishment of my goals.

Cofinanciado por:

UNIÃO EUROPEIA
Fundo Europeu
de Desenvolvimento Regional

Resumo

As infeções hospitalares originadas pela acumulação de bactérias em dispositivos médicos de interface, representam ainda um grande desafio para a sociedade. Estas infeções estão frequentemente relacionadas com o desenvolvimento de biofilmes, sendo difíceis de erradicar. O tratamento atual consiste em elevadas doses de antibióticos e na remoção do dispositivo. Os revestimentos anti-aderentes surgem como uma solução alternativa promissora. Polímeros naturais com boa relação custo-benefício e com propriedades não-tóxicas têm sido procurados como possíveis matérias-primas para o desenvolvimento dos referidos revestimentos. As cianobactérias são excelentes produtoras de substâncias poliméricas extracelulares (EPS) que podem ser libertadas para o meio (RPS), sendo por isso, facilmente isoladas. Estas substâncias possuem características particulares, nomeadamente uma ampla gama de conformações estruturais possíveis e um caráter aniónico, o que resulta num elevado potencial de aplicação. Assim sendo, o objetivo do presente trabalho foi desenvolver um revestimento polimérico anti-aderente baseado em RPS produzidos por uma cianobactéria, de forma a reduzir a adesão bacteriana e prevenir a formação de biofilme em dispositivos médicos, nomeadamente catéteres de poliuretano (PU). É de salientar que a maioria das estratégias, usadas neste trabalho para o desenvolvimento do revestimento (desde o crescimento da cianobactéria e a extração do polímero até à produção dos revestimentos) foram realizadas tendo em vista uma abordagem industrial. Para isso, a cultura de cianobactéria foi ampliada de biorreatores de 1 L para 5 L, de forma a aumentar a quantidade de RPS extraídos de uma maneira mais rentável. Além disso, diferentes meios de cultura foram testados, com o objetivo de otimizar os custos relacionados com o crescimento da cultura. Em relação ao desenvolvimento do revestimento, a ligação do revestimento baseado em RPS ao substrato (PU de grau médico) foi realizada utilizando três estratégias diferentes: polimerização de dopamina em camada de polidopamina (condições laboratoriais), ativação da superfície com plasma e ativação da superfície com ozono (condições industriais). De igual forma, foram testadas duas técnicas de revestimento, nomeadamente revestimento por imersão e por *spin-coating*. Para a avaliação da estabilidade dos revestimentos, foi realizado um ensaio de degradação acelerado. Finalmente, o desempenho anti-aderente foi testado usando espécies de bactérias clinicamente relevantes.

No geral, o aumento do volume da cultura da cianobactéria bem como o uso de diferentes meios de cultivação, não promoveram um efeito negativo no crescimento da cultura e na produção de RPS. Os resultados de caracterização do revestimento sugerem que diferentes técnicas de ativação de substrato foram capazes de ligar eficientemente o RPS a PU. Adicionalmente, todas as superfícies revestidas apresentaram uma forte redução na aderência bacteriana, mesmo na

presença de proteínas plasmáticas. Este trabalho representa um passo importante na translação de um revestimento anti-aderente polimérico de origem natural do ambiente laboratorial para um ambiente industrializável.

Abstract

Hospital-acquired infections arising from bacterial accumulation on indwelling medical devices are still a major challenge for society. These infections are frequently related to biofilm development, being difficult to eradicate. Current treatment consists in high antibiotic dosages and device removal. Anti-adhesive coatings arise as a promising solution to mitigate such infections. Cost-effective and non-toxic natural polymers have been pursued as possible raw materials in the development of such coatings. Cyanobacteria are excellent producers of extracellular polymeric substances (EPS) that can be released to the medium (RPS), being therefore easily isolated. These substances have particular features, namely wide range of structural conformations and anionic character, resulting in high application potential. Therefore, the aim of the current work was to develop a polymeric anti-adhesive coating based on RPS produced by a cyanobacterium, in order to reduce bacterial adhesion and prevent biofilm formation on indwelling devices, such as polyurethane (PU) catheters. Importantly, most of the techniques used here for the coating development (since cyanobacterial growth and polymer extraction to coating production) were performed envisaging an industrial approach. For that, cyanobacterium culture was scaled-up from 1 L to 5 L bioreactors, to increase the yield of extractable RPS. Also, different culture media were tested, in order to optimize costs related to culture growth. Regarding coating development, the linkage of the RPS-based coating to the substrate (medical grade PU) was performed using three different strategies: dopamine polymerization onto a polydopamine layer (laboratory settings), plasma surface activation and ozone surface activation (industrial settings). In addition, distinct coating techniques were performed, namely immersion- and spin-coating. For the assessment of coatings stability an accelerated degradation assay was performed. Finally, bacterial anti-adhesive performance was tested using clinically relevant species.

Overall, the cyanobacterial culture scale-up and the use of different culture media did not negatively affect bacterial growth and RPS production. Additionally, coating characterization results suggested that different substrate activation techniques were able to efficiently link RPS to PU. Moreover, all coated surfaces presented a strong reduction in bacteria adhesion, even in the presence of plasma proteins. This work represents a step forward in the translation of a natural derived polymeric anti-adhesive coating from the bench to more industrialized settings.

Index

List of figures

List of tables

Abbreviation and Symbols

AB	Alcian Blue
ATCC	American Type Culture Collection
ATR-FTIR	Fourier transformed infrared spectroscopy in attenuated total reflectance mode
ASN	Artificial sea water
AUTMS	Aminoundecyltrimethoxysilane
CAUTIs	Catheter-associated urinary tract infections
CCY	Culture Collection of Yerseke
CEMUP	Centro de Materiais da Universidade do Porto
CeNTI	Centre of Nanotechnology and Smart Materials
CFU	Colony forming units
Chl *a*	Chlorophyll *a*
CHT	Total carbohydrates
CRIs	Catheter-related infections
CVC	Central venous catheter
DA	Dopamine
DOPA	3,4-dihydroxy-L-phenylalanine
Draq5	Far red dye
DW	Dry weight
EPS	Extracellular polymeric substances
FTIR	Fourier transform infrared spectroscopy
HAIs	Hospital-acquired infections
ISO	International Organization for Standardization
MD	Medical devices
OCA	Optical contact angle
OD	Optical density
PBS	Phosphate-buffered saline
pDA	Polydopamine
PBS	Phosphate buffered saline solution
PEG	Polyethylene glycol
PP	Polypropylene
PTFE	Polytetrafluoroethylene
PU	Polyurethane
PUactO_2	O_2 plasma activated PU
PUactN_2	N_2 plasma activated PU

$PUactO_3$	Ozone activated PU
Rpm	Rotations per minute
RPS	Released polysaccharides
RT	Room temperature
SEM	Scanning electron microscopy
SD	Standard deviation
THF	Tetrahydrofuran
TrisHCl	Tris Hydrochloride
TSA	Tryptic soy agar
TSB	Tryptic soy broth
UTIs	Urinary tract infections
XPS	X-ray photoelectron spectroscopy

Poster presentations based on this Dissertation:

1) J. Cardoso, M.C.L. Martins, P. Tamagnini, F. Costa & R. Mota. "Development of an anti-adhesive coating based on a marine bacterium-produced polymer - towards industrial application" in "III Encontro Biotecnologia Medicinal/ 1st Iberian Congress on Medicinal Biotechnology" - Escola Superior de Saúde do Instituto Politécnico do Porto, Porto, Portugal (May, 2018).

Chapter 1

Introduction

1.1 - Motivation and aim

The use of indwelling devices, particularly catheters, is a very frequent medical procedure. Catheters are mostly used during surgeries, therapeutic delivery and fluids removal. Associated to its ubiquitous use, major complications associated with bacterial adhesion to its surface, subsequent biofilm formation and infection development are still to be more successfully addressed. Importantly, adhering bacteria present within biofilm environment are increasingly resistant to conventional antibiotic treatment that makes them very difficult to eradicate. Therefore, catheter-associated infections usually lead to the medical device removal/replacement, which aside from aggravating patient's overall health, also involves important economic burden.

The aim of the current work was to develop an anti-adhesive coating based on released polysaccharides (RPS) from a cyanobacterial strain, *Cyanothece* sp. CCY 0110, in order to reduce bacterial adhesion and prevent biofilm formation on indwelling devices, such as polyurethane catheters. Notably, most of the techniques used here for the coating development (since cyanobacterial growth and polymer extraction to coating production) were performed envisaging an industrial approach. The work herein reported can be divided in two major goals: (i) scaling-up of cyanobacterium culture and RPS extraction and (ii) optimization of coating application under industrial-like processes. Herein, cyanobacterium culture was scaled-up from 1 to 5 L bioreactors, and then the RPS secreted to the medium was extracted and purified. Also, different culture media were tested, in order to find the most cost-effective solution for culture growth. Regarding coating development, the linkage of the RPS-based coating to the substrate (medical grade polyurethane) was performed using three different strategies: dopamine polymerization onto a polydopamine layer (laboratory settings), plasma surface activation and ozone surface activation (under industrial settings). In addition, distinct coating techniques were performed, namely immersion-coating and spin-coating. The obtained

coated surfaces were characterized using complementary techniques (optical contact angle, scanning electron microscopy, x-ray photoelectron microscopy, Fourier transformed infrared spectroscopy in attenuated total reflectance mode and Alcian blue staining of RPS coated surfaces). Moreover, the obtained coated surfaces were challenged with an accelerated degradation assay being re-assessed afterwards. Finally, bacterial anti-adhesive performance of the coatings was also evaluated.

1.2 - Structure of the dissertation

In this dissertation, a complete literature review was prepared, exposing the most relevant and recent information on the subject in study.

The problem of indwelling medical devices-associated infections is introduced in Chapter 2, along with current used and researched strategies to minimize the issue.

Chapter 3 presents some of the surface characterization techniques used in this work. Theoretical fundaments, practical applications and operating mode of the different techniques are briefly exposed.

Materials and methods used can be found in Chapter 4 and the obtained results in Chapter 5. In Chapter 6 the discussion of the results is pursued in the light of current literature. In Chapter 7 the conclusions and future work are presented.

Chapter 2

Literature review

2.1- Bacterial infections associated to medical devices

Millions of lives are saved every day in modern healthcare, due to the use of medical devices that are increasingly applied in various areas of medicine. Nevertheless, the increased use of such foreign devices has given rise to serious complications, namely an increased risk of bacterial infections [1]. Recently, 722 000 hospital-acquired infections (HAIs) occurred in US intensive care facilities [2]. This corresponds to 1 in 25 inpatient admissions having an incidence of HAI that ultimately led to more than 75 000 patient deaths. A significant percentage of these HAIs (>25%) are medical devices-related (HAI-MD) [2]. Among the most common medical devices, indwelling polymer/polymer-coated devices (fig. 1) should be emphasised when considering their annual usage, infection and mortality rates [3].

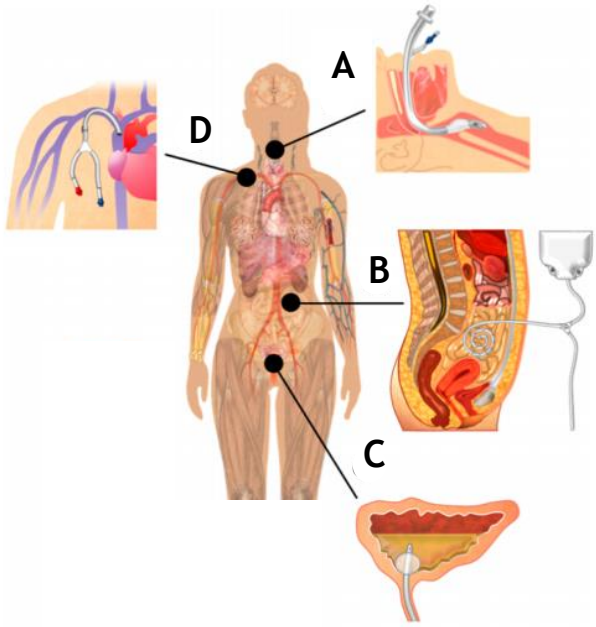

Fig. 1 - Commonly used polymeric or polymer-coated medical devices for temporary implantation. (A) endotracheal tubes, (B) peritoneal catheters, (C) urinary catheters, (D) central venous catheters. Adapted from [8].

Particularly, catheter-related infections (CRIs) significantly contribute to the increasing problem of nosocomial infections [3]. Indeed, there are nearly 80 000 central venous catheter (CVC) associated bloodstream infections that occur each year in US Intensive Care Units, with a 12–25% mortality rate [2]. The medical costs associated with these patient complications alone are estimated to be between $296 million to $2.3 billion, annually [2]. Additionally, urinary tract infections (UTIs) are believed to account for 30–40% of HAIs worldwide, and 80% are directly linked to catheterization, that is, catheter-associated UTIs (CAUTIs) [4].

There are different types of catheters according to specifications of the intended use: cardiovascular, urological, gastrointestinal, neurovascular and ophthalmic. The majority of catheters are made of flexible, durable, hydrophobic polymer materials, including polyurethane, silicon rubber and latex [5]. Although the biocompatibility of such materials, a major problem remains unsolved, that is, they are prone to bacterial attachment and consequent biofilm formation, which in turn results in CRIs [6]. Biofilms are remarkably resistant to both the host immune response and to systemic antibiotic therapies, and thus their development is the primary cause of medical devices-associated infections [7]. Biofilm formation on biomaterial surfaces (fig. 2) includes the following main steps: (1) initial reversible attachment of bacterial cells to the surface, (2) irreversible adhesion and synthesis of extracellular matrix, (3) microcolony formation, (4) biofilm maturation and differentiation, and (5) bacterial cell detachment with propagation of infection to other sites [8].

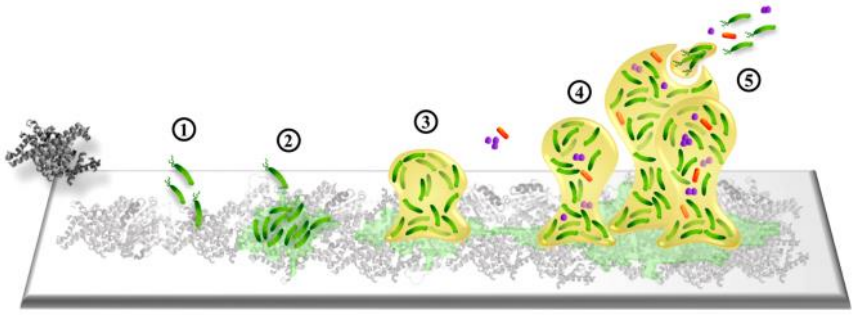

Fig. 2 - Stages of biofilm development: (1) bacterial attachment to the coated surface; (2) irreversible adhesion and synthesis of extracellular matrix; (3) formation of microcolonies; (4) maturation of biofilm architecture; (5) dispersion of bacteria. Adapted from [8].

Once applied, the medical device surface is first covered with a layer mostly composed of proteins, called a conditioning film, favouring bacteria–surface interactions [9]. In the first stage, bacteria and conditioning film protein interactions are mediated by weak attraction forces, such as Van der Waals and electrostatic charges, and are later strengthened by specific interactions involving bacterial adhesion proteins and extracellular biofilm matrix production [6]. Adhering bacteria can grow and divide, forming microcolonies that are considered the basic organizational units of a biofilm. Entrapment of other planktonic bacteria in the extracellular matrix also occurs, resulting in a multi-layered and mature biofilm. Under unfavourable environmental conditions, such as exhaustion of nutrients or overcrowding, sessile organisms can detach and become free-floating, or planktonic [10]. Importantly, biofilm bacteria are up to 1000-fold more resistant to antimicrobial agents compared to planktonic bacteria [6]. The decreased susceptibility to microbial agents within a biofilm arises from multiple factors, including physical impairment of diffusion of antimicrobial agents, reduced bacterial growth and metabolism rates, and local alterations of the microenvironment that may impair activity of the antimicrobial agent [11]. Furthermore, the proximity of bacterial cells within a biofilm can facilitate plasmid exchange and hence enhance the spread of antimicrobial resistance [10]. Therefore, when a medical device becomes colonized with a biofilm, the last resourced effective solution is often the removal of the infected material. Thus, the control of microbial adhesion and biofilm development on surfaces is a key issue in material science, as well as in medicine.

Infectious bacteria can be traced from several sources including the ambient atmosphere of the operating room, surgical equipment, clothing worn by medical professionals, resident bacteria on the patient's skin or mucosa, and bacteria already present inside the body [12]. Although sterilization and the use of aseptic techniques greatly reduces the levels of bacteria found in hospital settings, microorganisms are still found at the site of most indwelling devices, including catheters [12]. Regarding vascular catheters, bacteria can migrate from the skin (e.g. coagulase-negative *staphylococci*) or can reach the hub site via the hands of healthcare personnel (e.g. *Stenotrophomonas*, *Pseudomonas aeruginosa*, *Enterococci*, and

importantly *Staphylococcus aureus* and *S. epidermidis*) [13]. *S. epidermidis* is an opportunistic pathogen since it is found ubiquitously on the skin, having easier access to wounds, being known as a good-biofilm producer. However, *S. aureus* infections proceed rapidly and are generally more severe than *S. epidermidis* infections [12]. Regarding urinary tract catheters, the most common etiological agent is *Escherichia coli* [14], but other microorganisms are also frequently associated, namely *Enterococci spp.*, coagulase-negative *Staphylococci*, *P. aeruginosa*, *Proteus mirabilis* and *Candida spp.* [15]. Within the identified microorganisms, antimicrobial-resistance microorganisms are also common [16]. Indeed, the urine of patients with indwelling catheters is the major site of isolation of resistant gram-negative organisms, in both acute and long-term care facilities [17].

2.2- Strategies against bacterial adhesion and biofilm development

To reduce the frequency of HAI-MDs, many physicians resort to the administration of antibiotics prior to or immediately following device application [18]. However, this practice has proven to be insufficient and even contribute to the emergence of multiple antibiotic-resistant pathogens, which are globally spreading [7].

The development of biomaterials that can resist or prevent bacterial and protein adhesion, accumulation and consequent biofilm formation constitute a promising alternative approach to deal with bacterial infections [19]. Therefore, research has been focused on designing device surfaces to either kill microorganisms or repel them (fig. 3) [8]. Traditionally, these strategies can be divided into two categories: antimicrobial/killing and anti-adhesive/repelling biomaterials.

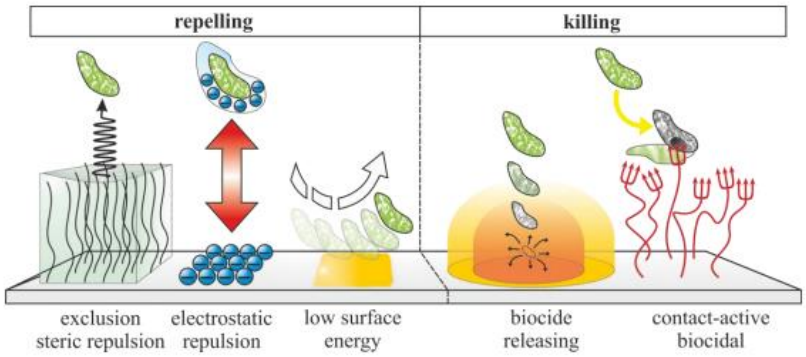

Fig. 3 – General mechanisms of antibacterial/killing and anti-adhesive/repelling surfaces. Adapted from [21].

In short, antimicrobial/killing materials are lethal to approaching microorganisms, whereas anti-adhesive materials prevent the adhesion of microorganisms and proteins.

Antimicrobial surfaces can be further classified as (i) antimicrobial- or biocide-releasing surfaces, when antimicrobials are released from the surface to target planktonic cells, or (ii) contact-killing surfaces, when the agents are directly immobilized on the surfaces to target approaching/attached cells [20]. However, antimicrobial approaches present some drawbacks. On the one hand, releasing strategies are short-termed, and the release of sub-inhibitory concentrations of the antimicrobial may contribute to microbial resistance, and on the other hand, contact-killing surfaces may have a longer scope of activity, but do not guarantee the detachment of dead bacteria, creating a favourable environment for further bacterial attachment [21].

Therefore, bacterial anti-adhesive strategies are gaining renewed interest. This type of approach is very promising since avoids the use of antimicrobials and its drawbacks. With the impairment of bacterial adhesion, the risk of biofilm formation and consequent infection can be reduced or even prevented [12]. In fact, even a slight delay in biofilm development could be beneficial, as it gives more time to the host immune system to act.

A common approach used in the development of anti-adhesive surfaces relies on the reduction of the attractive forces between bacteria and a biomaterial by optimizing the physico-chemical surface properties, always taking into account bacterial cell properties and environmental factors, such as the bulk medium composition (ionic strength, presence of organic substances) and flow conditions [20].

Physical modification of the surface topography or roughness, by elaborating smooth or micro-structured surfaces, for example, has proven to influence bacterial adhesion [22]. It is generally accepted that the smoother a surface is, the lower the probability of bacterial adhesion, although some studies have suggested otherwise [20]. Additionally, it seems that bacterial adhesion is enhanced when the features of the surface have dimensions or spacing similar to bacterial size (the micrometre scale) [23].

On the other hand, chemical modifications of surfaces, namely by the immobilization of polymeric coatings, may also promote bacterial anti-adhesive activity through a number of different mechanisms. The most widely investigated mechanism employs hydration forces and/or the steric repulsion [24]. When a protein approaches the surface, water molecules associated with the polymer chains are released, and the chains become compressed. The increase in enthalpy due to chain dehydration and the decrease in entropy due to chain compression are both unfavourable to bacterial adhesion and provide a thermodynamic basis for the anti-adhesive properties of the coating. While steric repulsion may play a role, it is now understood that hydrophilicity alone can impart surfaces that possess a tightly correlated water layer, which creates a physical and energetic barrier and causes interactions with approaching proteins or bacteria to become thermodynamically unfavourable. Moreover, superhydrophobic surfaces have also shown to repel bacteria [25]. It is also well known that adhesion of bacteria to negatively charged coated surfaces under physiological pH conditions may be affected by electrostatic repulsion forces since the net electrostatic charge of most bacterial cell walls is negative at neutral pH [26]. Additionally, low surface energy surfaces exploit the principals of

surface free energy and the work of adhesion to prevent bacterial attachment. When the surface free energy is reduced and the interfacial tension between the liquid and surface is high, the work of adhesion is minimized [8].

The immobilization of polymeric coatings comprising such anti-adhesive mechanisms can be one of the simplest, and potentially cost-effective ways to avoid biofilm formation, without changing the bulk (mechanical) properties of the biomaterials.

2.3- Coatings production and development strategies

Polyurethanes are among the best choices for biomedical applications considering their mechanical properties (due to their segmented polymeric character) - durability, elasticity, fatigue resistance and compliance - and their excellent blood and tissue compatibility [27]. However, in order to improve bacteria colonization resistance of polyurethane inert surfaces, these may be modified by a variety of strategies. The deposition of an anti-adhesive polymer layer as a coating is considered to be a promising approach to the prevention of adherent bacteria with consequent biofilm formation on biomaterials surface [28]. These coatings can be produced by simple and well described techniques such as dip/immersion-coating and spin-coating [29], [30].

Dip/immersion-coating is one of the simplest methods used for surface modification of a substrate, producing uniform thin coatings. This method is based on the immersion and withdraw of the biomaterial into a solution containing the dissolved coating material. After coating process, the solvent must be evaporated at room temperature or by heating to speed the process. Thickness of the coating is dependent on the features of the material to be deposited (viscosity, concentration and surface tension) and time of substrate immersion and withdraw from this solution [29].

Uniform ultrathin coatings can be produced by spin-coating. This technique involves deposition of a drop of a solution of the material to be coated into the centre of a substrate. After deposition, the substrate is spun at high speed. The coating material will be uniformly distributed by centripetal acceleration of the substrate at the same time that the solvent evaporates. Thickness of the coating will also depend on the characteristics of the material to be deposited including viscosity, concentration and surface tension, and the parameters chosen for the spin process, such as rotational speed and acceleration [30].

2.4- Coatings linkage to substrate strategies

To guarantee coating long-term stability, the linkage between the coating material and substrate must be optimized. Bond strength to the substrate material determines the stability of a coating [31]. This macroscopic property is controlled by: materials combination; type of interface zone; microstructure and process conditions; substrate type; and more importantly, pre-treatment. Pre-treatments activate and functionalize the substrate surface and therefore

substantially influence the bond between coating and substrate. This can be achieved through surface modifications, introducing novel functional groups and radicals that would serve as anchors for new added polymer layers. Examples of such surface modifications are plasma and ozone treatments or the application of an intermediate linker layer that is suitable for both coating and substrate [32], [33].

The application field of plasma technology is growing very fast. Moreover, increasing demands from industry encourage the continuous development of more efficient and more flexible plasma techniques, namely the cost-efficient atmospheric plasma activation [34]. Plasma is often referred as the fourth state of matter. It is a mixture of charged and neutral particles, such as atoms, molecules, ions, electrons, radicals and photons. In plasma treatments the incorporated groups change the surface properties, mainly the surface wettability and thus the surface energy, but also the surface roughness [35]. The work herein presented used both oxygen (O_2) and nitrogen (N_2) plasma treatments. Generally, O_2-plasma treatment leads to the introduction of oxygen-containing functional groups, such as carboxylic acid groups, peroxide groups (due to post-plasma reactions) and hydroxyl groups. Nitrogen, ammonia and N_2/H_2-plasmas introduce both N_2 and O_2-containing groups depending on whether the treated surface is maintained in inert atmosphere or if it is subsequently exposed to air [36], [37]. One major and important drawback of plasma treatment is the durability of the treatment effect. The surface undergoes a hydrophobic recovery after treatment and part of the generated effect is lost [32]. Nevertheless, plasma surface modification has several advantages that make this technology an excellent candidate for polymeric materials pre-treatment, such as not requiring the use of hazardous solvents and the possibility of modifying biomaterials surface features without affecting the bulk composition [38]. Additionally, when using the jet-plasma system it is possible to uniformly treat complex shaped materials [39], [40].

A second strategy implies the oxidization of the surface of a biomaterial by ozone [41]. Surface oxidation through this technique is a simple and easy to implement process that has been widely applied in the industry for improvement of inert polymers surface features. Ozone can be used as such, but it was found that a combination of ozone and UV irradiation can significantly increase the process kinetics [42], [43]. When a polymer is exposed to ozone, peroxides can be formed on the surface, as well as carbonyl and carboxyl groups that, depending on treatment period, may alter surface chemistry without affecting biomaterial bulk properties. However, additionally to the fact that ozone treatment can cause polymer degradation, this strategy can also show loss of treatment effect over time through surface hydrophobic recovery (similar to plasma treatments) [43].

Other approach for enhanced coating linkage to substrate is the application of an intermediate linker layer. In this work, a strategy inspired by the adhesive proteins secreted by mussels was used (fig.4(A)) [44].

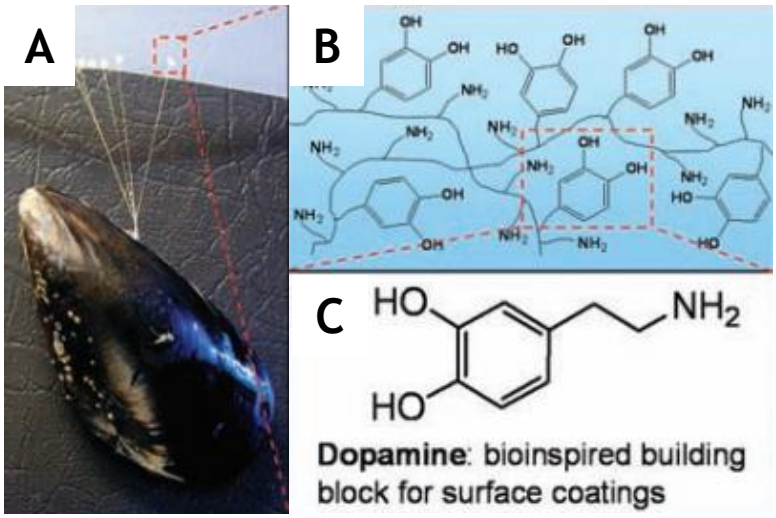

Fig. 4 - (A) Photograph of a mussel attached to commercial PTFE (polytetrafluoroethylene), (B) schematic simplified molecular representation of characteristic amine and catechol groups, (C) dopamine: contains both amine and catechol functional groups and is used as a molecular building block for polymer coatings. Adapted from [33].

Mussel's adhesive versatility has been reported to be related to 3,4-dihydroxy-L-phenylalanine (DOPA) and lysine amino acids (fig.4(B)) [45]. In addition to participating in reactions leading to bulk solidification of the adhesive, DOPA (fig.4(C)) is able to form strong covalent and noncovalent interactions with substrates [46]. Simple immersion of substrates in a dilute aqueous solution of dopamine, buffered to a pH typical of marine environments, results in spontaneous deposition of a thin adherent polymer film. The polydopamine coating is able to form on virtually all types of material surfaces and was found to be an extremely versatile platform for secondary reactions, such as the creation of functional organic ad-layers, namely alkanethiol monolayer, synthetic polymer and biopolymer coatings [33]. Therefore, polydopamine can also be used to enhance the attachment and stabilization of coatings that become independent from the interaction with the original substrate [44].

2.5- Synthetic and natural polymers for anti-adhesive coatings

The synthetic hydrophilic polymer, poly(ethylene glycol) (PEG), and its derivatives are the most widely used materials for anti-adhesive and antibacterial coating applications, given their resistance to protein adsorption, bacterial adhesion, non-immunogenicity and non-thrombogenicity [47]. Despite the attractiveness of PEG as an antifouling agent, low surface densities and susceptibility to oxidative damages [48] limit their antifouling capabilities over long-term applications. For these reasons, alternative hydrophilic polymers, such as polyglycerols, polyoxazolines and polyamides, with comparable protein resistance to PEG and improved oxidative stability, have been studied [127].

Numerous synthetic polymers with well-defined mechanical and degradation properties have been developed to meet the technological needs in the biomedical applications. However, these polymers may lack bioactivity and biocompatibility or cause toxicity [49]. Natural polymers arise as an alternative solution to design environmentally friendly and non-toxic materials. They present as major advantages: its renewable source, possibility of chemical functionalization to meet the technological needs and possible degradation into non-toxic residues [49]. Within natural polymers, polysaccharides are an important class with significant research interest for a variety of biomedical applications, including anti-adhesive coatings [50]. Nevertheless, polysaccharides also have some drawbacks including variation in the material properties based on the source, microbial contamination, uncontrolled water uptake, poor mechanical strength and, in some cases, unpredictable degradation pattern [49].

One of the most studied polysaccharides as a biofilm repelling coating is hyaluronic acid [51]. However, many commercial hyaluronic acid-based coatings currently available (e.g., Hydak® from Biocoat Inc., and Incert®-S from Anika Therapeutics Inc.) are mainly designed to minimize tissue attachment (e.g., post-surgery adhesions) on implants [50]. Heparin is another natural polysaccharide whose anti-adhesive properties have been extensively studied [7]. Heparin is also commonly used as an antithrombotic coating in implanted devices that are in contact with blood, in particular vascular catheters and stents. The Bioline Coating® from Maquet Cardiopulmonary GmbH, the Bioactive Surface CBAS® from Carmeda AB, and the Trillium® biosurface from Medtronic Inc., are some heparin-based antithrombotic coatings available on the market [50]. Dextran and its derivatives have also been widely investigated for their repelling properties limiting protein and animal cell adsorption/adhesion [48], but have been much more rarely tested as bacterial anti-adhesive coatings [52]. Recently, a sulphated polysaccharide from green algae (ulvan) have been covalently immobilized on titanium surfaces, which had been previously functionalized by the aminoundecyltrimethoxysilane (AUTMS) [53]. These modified surfaces were able to inhibit the initial adhesion of gram-positive (*S. epidermidis*) and gram-negative (*P. aeruginosa*) bacteria. Furthermore, the authors have demonstrated that such polysaccharide coatings affected the spreading of bacteria and could limit the bacterial colonization for a long time.

2.6- Extracellular polymeric substances from Cyanobacteria

Cyanobacteria are a large and widespread group of photoautotrophic microorganisms with the ability to combine oxygenic photosynthesis with typical prokaryotic features [54]. Certain strains also have the ability to fix atmospheric nitrogen, requiring minimal nutritional features [55]. In addition, cyanobacteria are able to synthesize extracellular polymeric substances (EPS), which can remain associated with the cell surface as sheaths, capsules and/or slimes, or be released into the surrounding environment as released polysaccharides (RPS).

In an industrial context, the use of cyanobacteria is advantageous compared to the use of plants or algae, as their growth rates are higher, their nutrient requirements are minimal,

and their growth conditions are easier to manipulate [56]. As a consequence, their overall production costs are lower [57], [58]. A deep knowledge regarding EPS production and properties, allow the optimization of the conditions that favours productivity and the desirable characteristics of the polymer. Previous studies revealed that the responses of cyanobacteria to changes in the culture conditions are strain-dependent [57]. These conditions include presence/absence of a nitrogen, phosphorous or sulphate source, temperature, aeration rate, light intensity, initial pH and growth phase [59]. In general, the chemical composition, the type and amount of the extracellular polysaccharides produced by a given cyanobacterial strain are stable features, mostly depending on the species and the cultivation conditions [60].

Cyanobacterial EPS are complex heteropolysaccharides, composed of up to 15 different monosaccharides: the hexoses, glucose, galactose, mannose and fructose; the pentoses, ribose, xylose and arabinose; the deoxyhexoses, fucose, rhamnose and methyl rhamnose; the acidic hexoses, glucuronic and galacturonic acid; and the aminohexoses, galactosamine, glucosamine and N-acetyl galactosamine [59], [61]. This composition contrasts with the polymers synthesized by other bacteria or microalgae, in which a lower number of different monomers, usually less than four, is found [59]. The available data on the monosaccharide composition of cyanobacterial EPS reveal some additional peculiar characteristics, such as the presence of one or two uronic acids, which were rarely found in the EPS produced by other microbial groups. In addition, cyanobacterial EPS contain sulphate groups, a unique feature among bacteria, but shared by the EPS produced by archaea and eukaryotes. Both sulphate groups and uronic acids contribute to the anionic nature of the EPS [62], [63].

In particular, RPS can be easily recovered from liquid cultures and, due to their physicochemical properties, are suitable for a variety of industrial applications, making cyanobacteria one of the most attractive sources of new polymers [59].

Considering the extensive literature claiming the potential for industrial exploitation of these biopolymers, it would be expected that technology transfer had already occurred. There are a significant number of patents available, covering the use of cyanobacterial polysaccharides in various industrial fields [64]. However, there are only a few industrial products derived from these biopolymers available in the market until now. One example is Spirulan, an acidic sulphated polysaccharide extracted from Spirulina (*Arthrospira platensis*) that is a filamentous cyanobacterium. In particular, Calcium Spirulan is a potent inhibitor of thrombin through heparin cofactor II [65] and is thought to enhance antiviral and anti-coagulation effects [66].

2.7- *Cyanothece* genus as strong EPS producer

Among EPS-producing cyanobacteria, several members of the *Cyanothece* genus are described as strong EPS producers [58], [59], [67]. In addition, strains belonging to this genus have been isolated from both freshwater and marine environments, allowing a given strain to be used for a specific purpose/environment. Nowadays, the study of marine strains is of

extreme importance since it allows the exploitation of an abundant resource, saltwater, compared to the scarcity of freshwater. *Cyanothece* sp. CCY 0110 is a marine N_2-fixing unicellular cyanobacterium isolated from coastal waters of Zanzibar and is among the most efficient EPS-producers. This cyanobacterium is capable of releasing most of the polymer to the culture medium (RPS) facilitating its isolation and recovery. An extensive characterization of the polymer have shown that, in agreement to what was previously described for other cyanobacterial polymers, *Cyanothece*'s RPS are complex macromolecules, composed of nine different monosaccharides including two uronic acids, peptides and sulphate groups [68]. Moreover, these RPS revealed to be versatile and promising for different areas, including bioremediation, as a biosorbent for heavy metals [69], to healthcare, as a vehicle for functional protein delivery [70]. Some of the features of this polymer resemble the ones found in other previously studied polysaccharides, and therefore, these RPS were studied in this work as a potential anti-adhesive coating.

Chapter 3

Surface characterization techniques

3.1- Optical contact angle (OCA)

The affinity that a surface has for a liquid/fluid is referred as wettability and can be quantified by the contact angle (θ). It is geometrically defined as the angle formed by a liquid drop at the three-phase boundary where the liquid, gas and solid meet (fig. 5(A)), or by the angle formed by an air bubble at the same three-phase boundary (fig. 5(B)) [71].

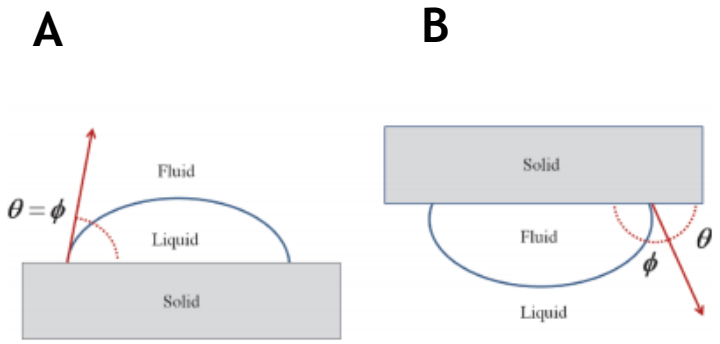

Fig. 5 – Contact angles θ observed with sessile drop (A) and captive bubble (B) measurement methods. The term fluid is applicable to a gas or an immiscible liquid with greater or lower density than the main liquid. Adapted from [71].

The behaviour of the liquid drop is dependent on cohesive forces of the liquid and adhesive forces between the liquid and the surface. When a drop is deposited on the surface, it spreads and the contact angle measurement is based on the balance between the force of attraction of the liquid molecules to each other (cohesive), and the attraction of the liquid molecules to the surface molecules (adhesive). There are several methods to determine a contact angle between a liquid and a surface [71]. In this work, both sessile drop and captive bubble methods were applied. In the sessile drop method, a drop of a liquid is placed on the

sample surface using a syringe and a video camera captures the image allowing the software to determine the contact angle between the drop and the surface by recurring to various curve-fitting methodologies such as Young-Laplace or Tangent [72].

Captive bubble method is based on a determined amount of air injected using a J-shaped needle into the liquid of interest to form an air bubble underneath the solid surface positioned facing downwards in a water tank (fig. 6). The test surface is positioned on the top of the test liquid and 2–3 mm above the needle end [73]. A captive bubble is formed when the air bubble floats upward and is "captured" by test surface. Contact angle θ, formed at the three phase contact line can be calculated from the drop profile of the bubble in a similar manner to the sessile drop method [74].

The contact angle measurement appears to be the simplest method to characterize surfaces [71]. This technique detects the topmost surface property with the analysis depth of approximately 1 nm or less being extremely sensitive.

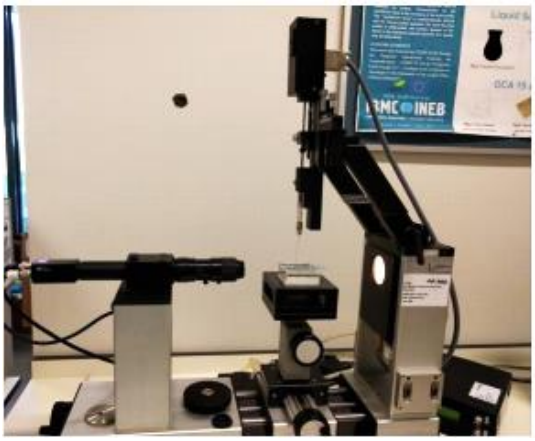

Fig. 6 – Goniometer equipment set up for captive bubble measurements.

3.2- Scanning electron microscopy (SEM)

Scanning electron microscopy (SEM) analyses the samples with a focused high energy electron beam in a raster scan pattern that interacts with the atoms on the surface, acquiring information about sample's topography and composition (fig. 7). A variety of signals are produced by electron-sample interactions. These signals include secondary electrons, backscattered electrons, diffracted backscattered electrons, photons, visible light and heat. The signals that derive from these interactions contain information about the sample's morphology and topography, chemical composition and crystalline structure [75], [76].

Fig. 7 - Scanning electron microscopy equipment at Centro de Materiais da Universidade do Porto.

3.3- X-ray photoelectron spectroscopy (XPS)

X-ray photoelectron spectroscopy (XPS) also named as electron spectroscopy for chemical analysis (ESCA) (fig. 8) is based on photoelectric effect. When an X-ray is focused on a sample, it causes emission of core-level electrons in the atoms near the surface [77]. The kinetic energies of the emitted electrons are measured by the XPS detector and subtracted from the known energy of the X-rays used, allowing the determination of the binding energies of the respective atoms. Since each element has a unique range of binding energies, individual peaks in the spectrometer signal can be attributed to the presence of certain elements. The areas under each of the peaks also correlate to the respective ratios of those elements on the sample surface and can therefore be used for relative quantitative compositional analysis. XPS is particularly useful for identifying and confirming the presence of a surface modification on a substrate [78]. XPS typically measures the average surface chemistry up to a depth of approximately 10 nm [131]. Therefore, XPS is less surface sensitive than the contact angle measurement.

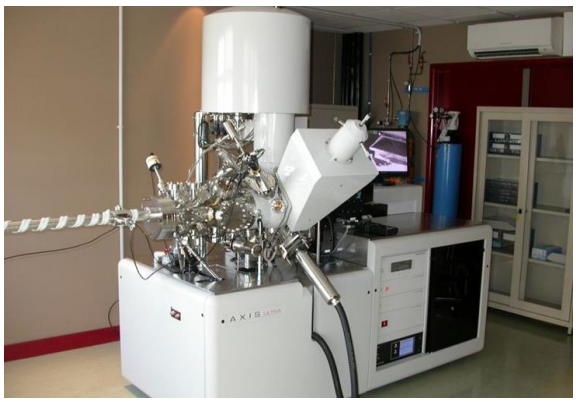

Fig. 8 – X-ray photoelectron microscopy equipment at Centro de Materiais da Universidade do Porto.

3.4- Fourier-transform infrared spectroscopy (FTIR)

Fourier-transform infrared spectroscopy (FTIR) is a spectroscopic technique based on the use of infrared beam to analyse the chemical functionalities present in a sample. When an infrared (IR) beam hits a sample, chemical bonds stretch, contract and bend, causing it to absorb IR radiation in a defined wavenumber [79]. This technique provides information about the molecular structure, inter and intramolecular interactions, crystallinity, conformation and orientation of molecules. Infrared spectroscopy can also be used in attenuated total reflection mode (ATR-FTIR) (fig. 9). In this mode, the incident IR beam first passes through a ZnSe, Ge, or diamond crystal, improving the surface sensitivity of the technique. Total reflection occurs at the interface between the sample and this internal reflection element, but instead of reflecting totally, a fraction of the incident IR enters into the sample in a form of electromagnetic wave with an exponentially decreasing magnitude and with a penetration depth between 0.2 and 5 μm, being the less sensitive technique used here [80].

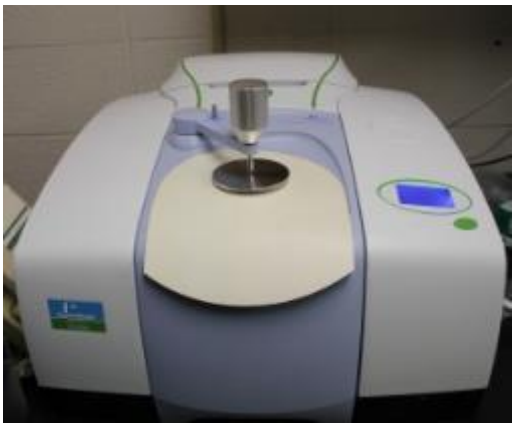

Fig. 9 – Fourier transformed infrared spectroscopy in attenuated total reflectance mode (ATR-FTIR) equipment.

Chapter 4

Materials and methods

4.1- *Cyanothece* sp. CCY 0110 cultivation and RPS production

4.1-1. *Scale-up of Cyanothece* sp. CCY 0110 culture and growth conditions

The cyanobacterium *Cyanothece* sp. CCY 0110 (Culture Collection of Yerseke, the Netherlands) was grown in 1 L and 5 L bioreactors (DWK Life Sciences) containing 700 mL and 3.5 L of ASNIII medium [81], respectively (fig. 10).

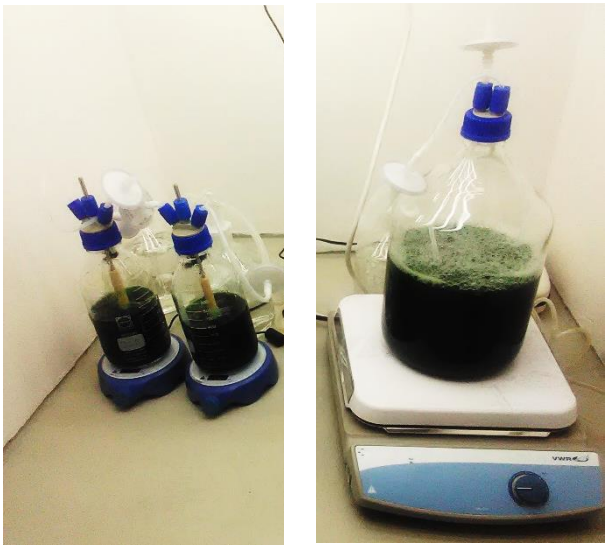

Fig.10 - Cultures of *Cyanothece* sp. CCY 0110 in 1 L (left), and 5 L (right) bioreactors.

regimen, with magnetic stirring (200 rpm) and with aeration (1.2 L min^{-1}). Two replicates of cultures grown in 5 L bioreactor were performed.

4.1-2. *Cyanothece* sp. CCY 0110 growth measurements and carbohydrate content determination

i) Optical microscopy and Alcian blue (AB) staining

Cells were observed using an Olympus X31 light microscope (Olympus) and micrographs were acquired with an Olympus DP25 camera and the Cell B software (Olympus). Cells were also stained with Alcian Blue at 0.5% (w/v in 50% ethanol) for the visualization of acid carboxylated and sulphated polysaccharides [82].

ii) Optical density (OD)

OD measurements were performed once every two-weeks at 730 nm [83] using a UVmini-1240 UV-vis spectrophotometer (Shimadzu Corp.). For OD measurements, 1 mL of culture were collected and diluted (OD <1) using type II water.

iii) Dry weight (DW)

DW measurements were performed in triplicates on the first and last days of culture growth. 5 mL of culture were collected and centrifuged for 10 min at 5000 rpm and room temperature (RT). After centrifugation, pellet was resuspended in type II water and transferred to previously dried (overnight at 55 ºC) and weighted tubes. New centrifugation at maximum speed using a mini-spin plus microcentrifuge (Eppendorf) was then performed. Afterwards, pellets were dried for 24 h at 55 ºC. After 24 h period, tubes were weighted and the DW was calculated (DW: weight (g) of tube with pellet, 24 h incubation – weight (g) of tube without pellet, 0 h incubation).

iv) Specific growth rate

Specific growth rate (μ) was calculated from the slope of the semi-logarithmic plot of growth expressed as OD_{730nm} versus time [84].

$$\mu = \frac{1n\left(\frac{X_t}{X_o}\right)}{t - t_o}$$

where μ = specific growth rate (day^{-1}), Xt = optical density (nm) at time t, Xo = initial optical density (nm) at t = 0, and t = time (days).

v) Carbohydrates content determination

Carbohydrate content determination was performed in triplicates, on the first and last days of culture growth. 20 mL aliquots of the culture were placed into dialysis membranes (12–14 kDa of molecular weight cut-off; Medicell International Ltd) and dialyzed against a minimum of 10 volumes of type II water for 24 h with continuous stirring. Total carbohydrate content was quantified spectrophotometrically at 488 nm by the phenol-sulphuric acid assay [85]. The amount of carbohydrates released to the culture medium (RPS) was also determined, starting by centrifuging 5 mL of culture for 15 min at 5000 rpm, RT, and measuring the carbohydrate content of the supernatant by the method mentioned above. Total carbohydrate and RPS contents are expressed as mg per L of culture.

4.1-3. RPS isolation and purification

For RPS isolation, *Cyanothece* sp. CCY 0110 culture was grown until an $OD_{730\ nm}$ of approximately 3.5-4. After that, RPS isolation from half of the culture was immediately performed, while the other half was maintained in the culture chamber for another week prior to RPS isolation. This was due to technical limitations in processing the whole volume of the culture. Briefly, *Cyanothece* culture was dialyzed (12-14 kDa of molecular weight cut-off; Medicell International Ltd) against a minimum of 10 volumes of type II water for 48 h in continuous stirring. Cells were then removed by centrifugation at 20 000x*g* for 15 min at 4 ºC and supernatant were precipitated with 2 volumes of absolute ethanol (Aga UN1170) at 4 ºC, overnight. RPS were then collected with sterile metal forceps, dissolved in type I water, precipitated once more and lyophilized (VirTis BenchTop Pro with Omnitronics™, SP Scientific) [68]. After lyophilisation, RPS polymer was milled (A10 basic, IKA) and stored in a desiccator.

4.1-4. Test of culture media with reduced cost

To evaluate the influence of different culture media on *Cyanothece* sp. CCY 0110 growth and RPS production, 500 mL Erlenmeyer flasks were used with 300 mL of the following media (fig. 11):

- ASNIII as control;
- ASNIII with sea water - sea water replacing type II water and sodium chloride;

- NutriBloom Plus with sea water - 1% (v/v) of commercial culture medium for microalgae cultivation enriched with vitamins (PhytoBloom by Necton) in sea water.

All cultures were grown with the previously described conditions on section 4.1-1. (with the exception of aeration) in three replicates. In addition, culture growth and RPS production was evaluated every two-weeks using the parameters and methods as previously described (section 4.1-2.).

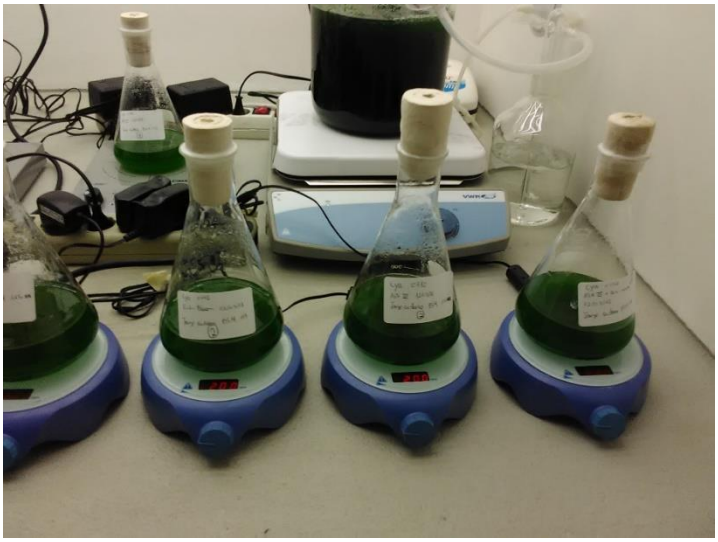

Fig.11 - *Cyanothece* sp. CCY 0110 cultures grown in 300 mL of three different media: ASNIII, ASNIII with sea water and NutriBloom Plus with sea water.

4.2- RPS coating development

4.2-1. Preparation of polyurethane surfaces (PU)

Medical grade polyurethane (fig. 12) pellets (PU, pellethane 2363-80AE, Velox) were initially sonicated (15 min) twice with hexane (EMSURE ACS n-Hexane, Merck) and once with 99% ethanol (Enzymatic) to eliminate silicone casing of extrusion fabrication process. This step was repeated twice. Then, PU pellets were left to dry overnight in the hood and subsequent 24 h in the vacuum oven at RT (Trade Raypa) for complete evaporation of the solvent. Thereafter, PU was dissolved at 12.5% w/v in tetrahydrofuran (THF) (EMSURE ACS, Reag. pH Eur tetrahydrophuran, Merck) and 40 mL of the solution were casted onto clean glass Petri dishes of 140 mm of diameter. These petri dishes were covered with aluminium foil and small holes were punched with a needle to allow a very slow evaporation of THF [86]. Films were left to dry in the hood for 48 h and an extra 24 h in the vacuum oven at 40°C to guarantee complete THF evaporation. PU films were then cut into small disks of 14 mm of diameter (PU disks) and

washed subsequently in hexane, 99% ethanol, and 3 times with type II water (5 min sonication each) to remove possible debris resultant from the cutting process. Finally, PU films were dried and stored with argon and protected from light.

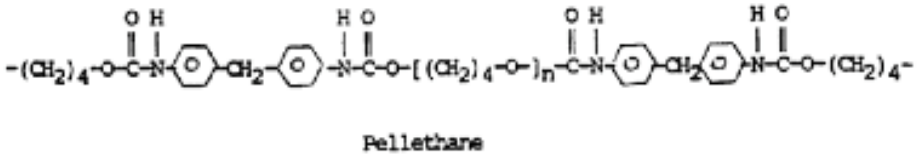

Pellethane

Fig. 12 - Pellethane chemical structure. Adapted from [126].

4.2-2. Substrate activation pre-treatments

Surface activation of PU films for efficient coating linkage and stability, were performed using three different strategies: polydopamine (pDA) layer application, oxygen (O_2) or nitrogen (N_2) plasma activation and ozone (O_3) activation. Plasma and ozone treatments of PU surfaces were performed at CeNTI (Centre of Nanotechnology and Smart Materials) using the samples described in section 4.2-1.

4.2-2.1. Polydopamine layer application (PU+pDA)

PU disks were incubated with 1 mL of dopamine hydrochloride (Sigma Life Sciences) solution (2 mg/mL) in 10 mM tris-HCl buffer (pH 8.5) at 70 rpm agitation, RT using a 24 well cells suspension plate (Corning Incorporated). Two different incubation periods were tested: 18 and 24 h. After incubation, samples were sonicated twice with tris-HCl buffer and once with type I water in order to remove loosely attached polymer. Finally, pDA coated PU surfaces were dried with argon for surface characterization or coating application.

4.2-2.2. Plasma O_2/N_2 treatment (PUactO_2/N_2)

An industrial atmospheric plasma system (U2ERX2-2200-Sigma Technologies International, located at CeNTI) (Fig. 13), with an estimated maximum power of 15 kW, was used for the surface activation of PU films. Films were exposed simultaneously to an argon flow rate of 15 L/min and an O_2 or N_2 flow rate of 0.45 L/min, depending on the respective selected reactive gas for plasma treatment. Surfaces were exposed to plasma for less than 1 s.

Different process parameters combinations of applied power (kW) and frequency of motor rotation (Hz) were tested for the optimization of plasma surface treatment:

- Parameters 1 (P1): 7.5 kW, 3.3 Hz;
- Parameters 2 (P2): 11.3 kW, 3.3 Hz;
- Parameters 3 (P3): 15.0 kW, 1.1 Hz.

Fig. 13 - Plasma equipment at CeNTI.

After plasma surface activation, PU films were transported back to the i3S laboratory in a low density polyethylene (PE-LD) bag (Enzymatic) and then cut into 14 mm diameter disks for surface characterization or for RPS coating application.

4.2-2.3.Ozone treatment (PUactO_3)

An industrial ozone generator (Fisher Ozon-generator 500, located at CeNTI) (Fig. 14) was used for the ozone surface modification procedure of PU films. Films were exposed to an O_3 atmosphere inside a 10 L bioreactor (Paralab) during 15 min followed by 10 min of oxygen in order to remove reminiscent ozone on PU surfaces and minimize the risk excessive reactivity and prevent personal damage. After ozone surface activation, PU films were transported back to the i3S laboratory as described for plasma surface activation.

Fig. 14 - Ozone generator equipment (left) and 10 L bioreactor (right) at CeNTI.

4.2-3. RPS coating application

4.2-3.1. Preparation of RPS solution

RPS solution (fig. 15) was prepared by hydrating the RPS polymer 0.5% (v/v) with type II water, for 24 h with magnetic stirring, and subsequently autoclaved at 110°C for 30 min.

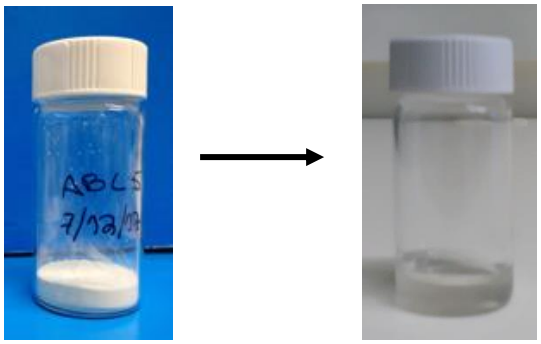

Fig. 15 - Preparation of RPS solution for consequent coating procedures: milled RPS before (left) and after (right) 24 h hydration with type II water.

4.2-3.2.RPS coating application by spin-coating

RPS coating deposition on top of pre-treated PU disks was performed by spin-coating (WS-650MZ-23NPP/LITE, Laurell Technologies corporation) (fig. 16). Briefly, 80 µL of RPS solution was added to the centre of samples and span for 1 min at 9000 rpm with 1500 acceleration. Obtained coatings were dried in a vacuum oven for 1 h at RT. Samples were then sonicated for 1 min in type I water dried and stored with argon, protected from light.

4.2-3.3. RPS coating application by immersion-coating

Pre-treated PU disks were placed on a 24-well plate for the RPS coating production by immersion (fig. 16). One mL of RPS solution was added to each well and incubated for 1 h at RT. After incubation period samples were washed thrice with type I water to remove non-attached polymer. Finally, surfaces were dried and stored with argon and protected from light for further surface characterisation.

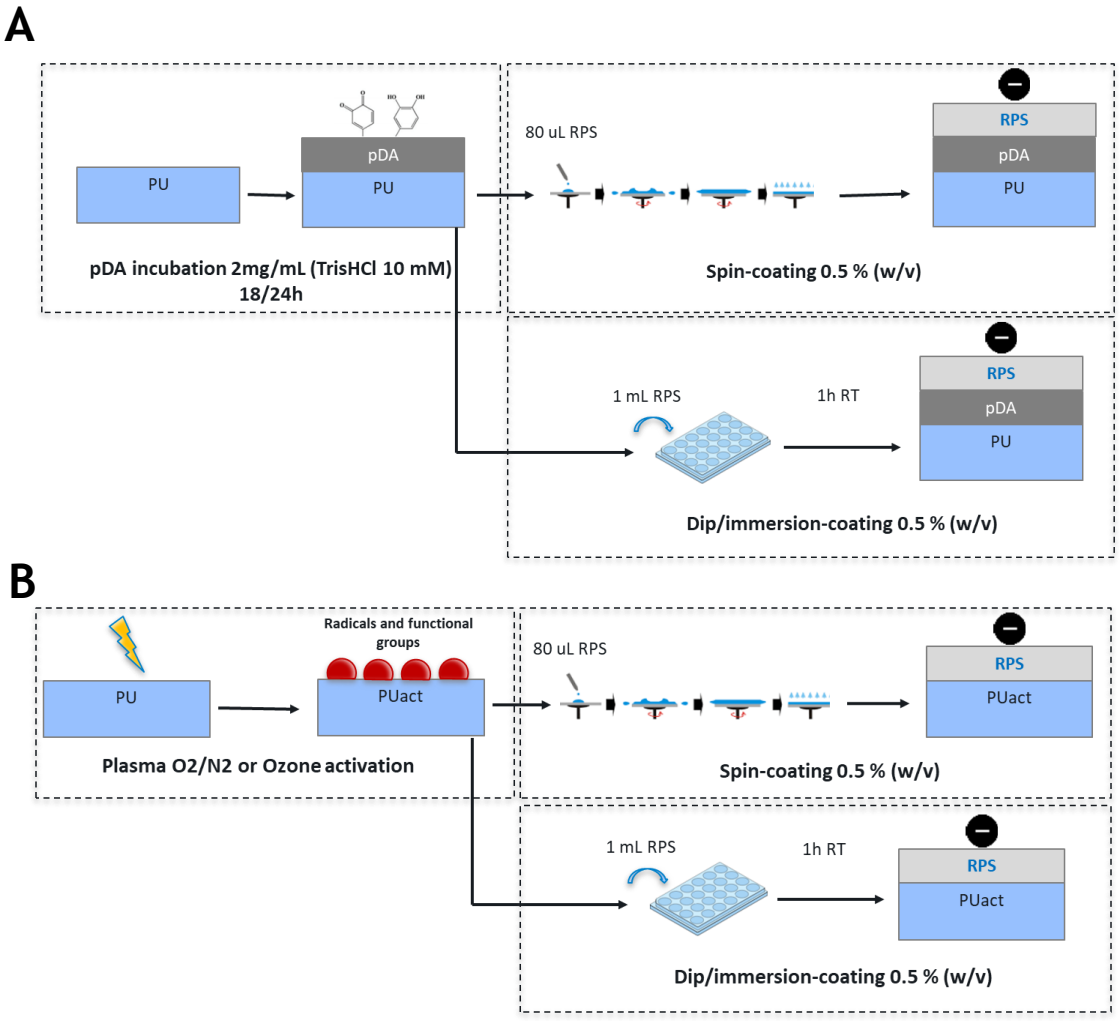

Fig. 16 - Schematic representation of RPS spin- dip/immersion-coating production via (A) pDA layer application and (B) plasma or ozone treatments.

4.2-4. Surface characterization

Several surface characterization techniques were applied to the samples at each stage of modification: optical contact angle (OCA), scanning electron microscopy (SEM), x-ray photoelectron spectroscopy (XPS) and Fourier-transform infrared spectroscopy in attenuated total reflectance mode (ATR-FTIR). Additionally, surface staining with Alcian Blue was also conducted using unmodified and RPS coated surfaces.

Before measurements, samples were previously dried on vacuum oven at RT for 1 h, particularly for OCA and ATR-FTIR measurements.

4.2-4.1. Optical contact angle (OCA)

Both sessile drop and captive bubble methods were applied to study wettability modifications regarding RPS-coated, pre-treated and unmodified PU surfaces. Contact angle measurements at CeNTI were performed using a Theta tensiometer from Attension (Biolin Scientific), while the measurements at i3S were performed using a system from Data Physics, model OCA 15, equipped with a video CCD-camera and SCA 20 software.

For sessile drop method, a drop of 4 µL type II water was applied on pre-dried samples (as explained in section 2.4). For captive bubble method, a 10 µL air bubble was applied on surfaces that were pre-immersed in type II water for 5 min. For both methods, droplet profiles were fitted using the Young-Laplace or Tangent mathematical function in order to calculate the contact angle [11]. Generally, three replicates of each PU modification stage were used. Three measurements were made per replicate. Droplet/bubble profile images for further contact angle calculation were acquired immediately at the contact moment between droplet/bubble and substrate surface.

i) Hydrophobic recovery of plasma and ozone treated surfaces

Aging and hydrophobic recovery of plasma and ozone-activated surfaces was evaluated by storing samples throughout 3 days in Ar environment. Sessile drop measurements were performed every 24 h. A preliminary captive bubble assay regarding the monitoring of O_2/N_2 plasma activated surfaces under different storage environments (Ar and type I water) for 3 days was also conducted. Captive bubble measurements were performed every 24 h.

4.2-4.2. Scanning electron microscopy (SEM)

SEM surface characterization was performed using a high-resolution FEI QUANTA SEM equipment with X-ray Microanalysis at CEMUP – Centro de Materiais da Universidade do Porto. Micrographs of the surfaces were taken using an electron beam intensity of 5 kV (accelerating

voltage) and a magnification of 1000x and 5000x. To increase the surface conductivity, samples were previously sputtered with gold/palladium (Au/Pd) for 60 s and 15 mA current using the SPI module sputter coater equipment.

4.2-4.3. X-ray photoelectron spectroscopy (XPS)

XPS measurements were performed using a Kratos Axis Ultra HSA spectrometer with an Al monochromatic X-ray source operating at 15 kV (90 W). Photoelectrons were analysed at 100 Å from the outermost layer and 70° take-off angle. Survey scans were acquired with a pass energy of 80 eV.

4.2-4.4. Fourier-transform infrared spectroscopy in attenuated total reflectance mode (ATR-FTIR)

ATR-FTIR analysis of unmodified and coated PU surfaces was performed on a FTIR spectrophotometer from Perkin Elmer, model 2000, coupled with an ATR accessory (split-pea) and a nitrogen-cooled mercury cadmium telluride (MCT) detector. Data was collected at 4 cm^1 resolution with a total of 32 scans.

4.2-4.5. Surface Alcian blue (AB) staining

Unmodified and RPS coated PU surfaces were subjected to AB staining. Briefly, samples were placed on a 24-well plate and stained with 500 µL of AB at 0.5% (w/v in 50% ethanol) for visualization of acid carboxylated and sulphated polysaccharides present on RPS-polymer composition. After that samples were washed thrice with type I water and dried with Ar.

4.2-5. RPS coating degradability evaluation

RPS-based coatings obtained through the different linkage strategies, were subjected to accelerated coating degradation assay according to the ISO 10993-13 (2009) (Biological evaluation of medical devices – Identification and quantification of degradation products from polymeric medical devices) adapted protocol. Surfaces were placed on 20 mL polypropylene (PP) flasks and were exposed to the following conditions:

1. Freshly prepared RPS coating (RPS control) - Day0;
2. RPS coating incubated 7 days at 45 °C - Day7 45 °C;
3. RPS coating incubated 1 h at RT in PBS (pH 7.4) - 1h RT (pH7.4);
4. RPS coating incubated 1 h at RT in acetate buffer (pH 5) - 1h RT (pH5);
5. RPS coating incubated 7 days at 45 °C in PBS (pH 7.4) - Day7 45 °C (pH7.4);
6. RPS coating incubated 7 days at 45 °C in acetate buffer (pH 5) - Day7 45 °C (pH5);

At the end of the assay, samples were washed thrice with 3 mL type I water for 5 min at 70 rpm, dried and stored with argon for surface characterization (OCA measurements).

4.2-6. RPS coating anti-adhesive performance evaluation

Bacterial anti-adhesive performance of the RPS-based coatings obtained through the different linkage strategies were evaluated following the ISO 22196 (2011) (Measurement of antibacterial activity on plastics and other non-porous surfaces) adapted protocol. All experiments were performed on a flow chamber to prevent cross-contamination. Three different bacteria were chosen to evaluate RPS coating anti-adhesive performance: Gram-positive *Staphylococcus aureus* (ATCC 49230) and *S. epidermidis* (ATCC 35981) and Gram-negative *Escherichia coli* (ATCC 25922). Briefly, 5 μL of a bacterial inoculum adjusted to $1.8x10^6$ CFU/mL on tryptic soy broth (TSB, Merck) was added onto previously sterilized samples (2x 15 min 70% ethanol + 2x 15 min type I water). The influence of plasma proteins on bacterial adhesion was investigated by adding blood plasma (kindly supplied by Hospital de São João) at 1% (v/v) into bacterial inoculum. Inoculated samples were then covered with a 9 mm diameter polypropylene (PP) film to promote the contact between bacteria and the sample surface. Samples were then incubated for 24 h under static conditions at 37 °C and high moisture conditions. After 24 h incubation period, samples were washed thrice with 1 mL of PBS, for the removal of loosely bond bacteria. Surface adhered bacteria were then fixed with paraformaldehyde at 4% during 20 min. After fixation, samples were rinsed thrice with PBS and bacteria were stained with 5 μM of a far-red fluorescent live-cell permeant DNA dye (DRAQ5, Biostatus limited) during 15 min. Samples were then rinsed twice with PBS and placed upside down to a black IBIDI 24-well μ-plate, filled with 500 μL of PBS in each well. Images of 9 fields (area of each field: ~0.126 mm^2) per sample were acquired using the high-content screening microscope IN Cell Analyzer 2000 (GE Healthcare Life Sciences) in the Cy5 (705 nm) channel through 3-D deconvolution, with a Nikon 40x/0.95, PlanApo, corr collar 0-11-0.23, CFI/60 Lambda objective. Nine stacks per field with different z's (z-step of 1.5 μm) were acquired and then collapsed on INCELL Developer program (Collapse protocol). Quantification of adhered bacteria was performed using ImageJ software and was expressed as the number of bacteria/mm^2.

4.2-7. Statistical analysis

Statistical analysis was performed by firstly assess D'Agostino Pearson omnibus normality test. Depending on the data normality assessment non-parametric Kruskal-Wallis, ANOVA or Paired t tests were used. Data is expressed as mean ± standard deviation (SD) and significant differences are expressed as: * p value ≤ 0.05; ** p value ≤ 0.01; *** p value ≤ 0.001; **** p value ≤ 0.0001.

Chapter 5

Results

5.1- *Cyanothece* sp. CCY 0110 cultivation and RPS production

5.1-1. Effect of *Cyanothece* sp. CCY 0110 culture scale-up on growth and carbohydrates production

In order to evaluate the translation of the cyanobacterium *Cyanothece* sp. CCY 0110 (hereafter *Cyanothece*) culture establishment towards an industrial level, a scale-up from 1 L to 5 L bioreactors (5-fold scale-up) using previously described conditions (see section 4.1-1) was performed and then the culture growth and carbohydrate production were evaluated. Additionally, the influence of different culture media on *Cyanothece* growth and carbohydrates production was also evaluated with the intuit of ascertain the possibility of reducing medium costs.

By optical microscopy is possible to observe the unicellular morphology characteristic of this cyanobacterial strain (fig. 17(A)). In addition, the high production of acid carboxylated and sulphated polysaccharides (more particularly released polysaccharides - RPS) by this strain were observed by the Alcian blue staining (fig. 17(B)).

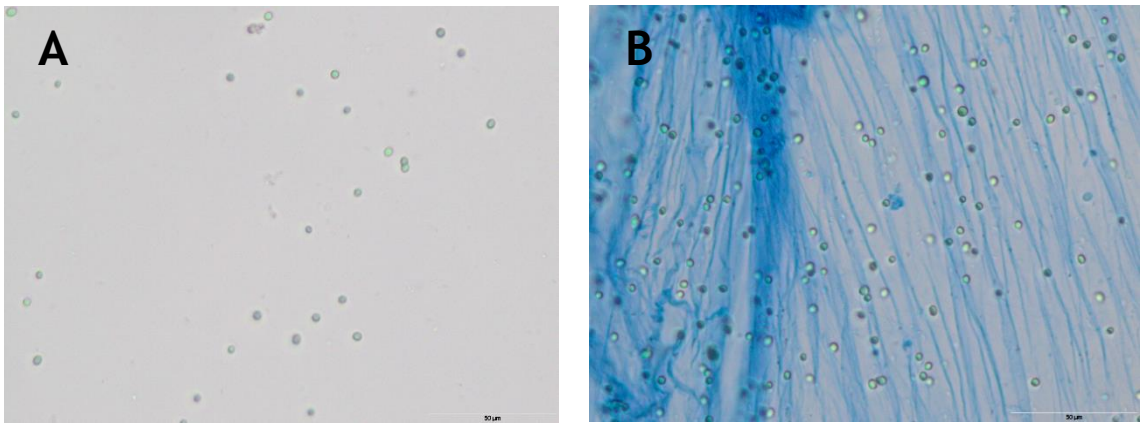

Fig. 17 - Light micrographs of *Cyanothece* sp. CCY 0110 culture: (A) without stain; (B) released polysaccharides stained with Alcian Blue.

Culture growth was evaluated by monitoring different parameters, such as optical density (OD_{730nm}) and dry weight (DW). As it can be seen in the data presented in fig. 18, both parameters followed the same pattern. There was an increase in both OD and DW concentration during the 70 days revealing a linear and slow growth of *Cyanothece* over time. Therefore, as an example, it is possible to stipulate that an $OD_{730\ nm}$ of 3.6 corresponds to a DW value of 750 mg/L of culture grown in ASNIII medium. Additionally, specific growth rate (using OD_{730nm}) of culture scale-up was also calculated for growth evaluation. Achieved specific growth rate was μ =0.0071 day^{-1}.

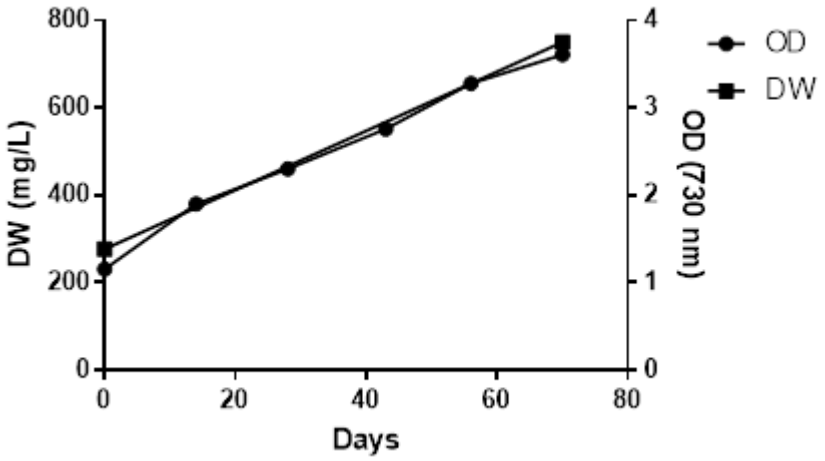

Fig. 18 - Growth of *Cyanothece* sp. CCY 0110 expressed as OD_{730nm} and mg of DW per L of culture. Cultures were grown in 5 L bioreactors with ASNIII medium, at 25 ºC, a 16 h light (30 µmol photon m^{-2} s^{-1})/8 h dark regimen, with aeration (1.2 L min^{-1}). The values are means ± standard deviations (n =2).

To determine if the carbohydrate production was affected by the culture scale-up, total carbohydrates (intracellular and extracellular carbohydrates including RPS) and RPS contents were measured. Fig. 19 strongly suggests that total carbohydrates (CHT) and RPS content (mg) per L of culture followed the same pattern, having an increase of about 2 to 3-

fold from the beginning until the end of selected culture growth period. In comparison to *Cyanothece* growth, carbohydrates content also followed the same pattern as OD and DW during cultivation period. Additionally, the analysis of the percentage of the RPS present in the culture suggested a constant level of this polysaccharides over time, representing approximately 75% of CHT in the beginning of the experience and approximately 81% after 70 days of cultivation.

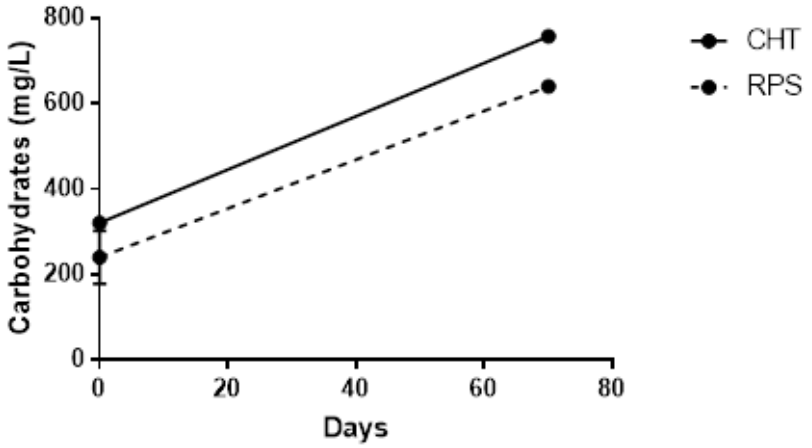

Fig. 19 - Total carbohydrates (CHT) and released polysaccharides (RPS) content expressed as mg per L of ASNIII culture (mg/L). Cultures were grown in 5 L bioreactors with ASNIII medium, at 25 ºC, a 16 h light (30 µmol photon m^{-2} s^{-1})/8 h dark regimen, with aeration (1.2 L min^{-1}). The values are means ± standard deviations (n = 2).

The amount of carbohydrates present in the culture was also normalized to DW concentration in order to evaluate the production of carbohydrates at the cell level. As it can be seen in Table 1 the values of total carbohydrates and RPS content per mg of DW were similar at the beginning and the end of the cultivation period. Total amount of produced and isolated RPS after isolation and purification processes was 3.3 g that corresponds to approximately 1.1 g per L of culture.

Table 1 - Total carbohydrates (CHT) and released polysaccharides (RPS) content

Days	CHT (mg/mg DW) [a]	RPS (mg/mg DW)
0	1.16 ± 0.02 [b]	0.87 ± 0.23
70	1.01 ± 0.00	0.82 ± 0.02

[a] content expressed as mg of carbohydrates per mg of dry weight.
[b] The values are means ± standard deviations (n = 2).

5.1-2. Effect of different culture media with reduced cost on *Cyanothece* sp. CCY 0110 growth and carbohydrates production

To evaluate the influence of different culture media on *Cyanothece* growth and carbohydrate production, the following media were tested: ASNIII (control), ASNIII with sea water and NutriBloom Plus with sea water.

Culture growth was evaluated using the same parameters as the ones used for growth evaluation of 5-fold culture scale-up. The data presented in fig. 20 strongly suggests that OD and DW concentration per L of culture followed the same pattern regarding all types of culture media tested, revealing a linear and slow growth of *Cyanothece* over time.

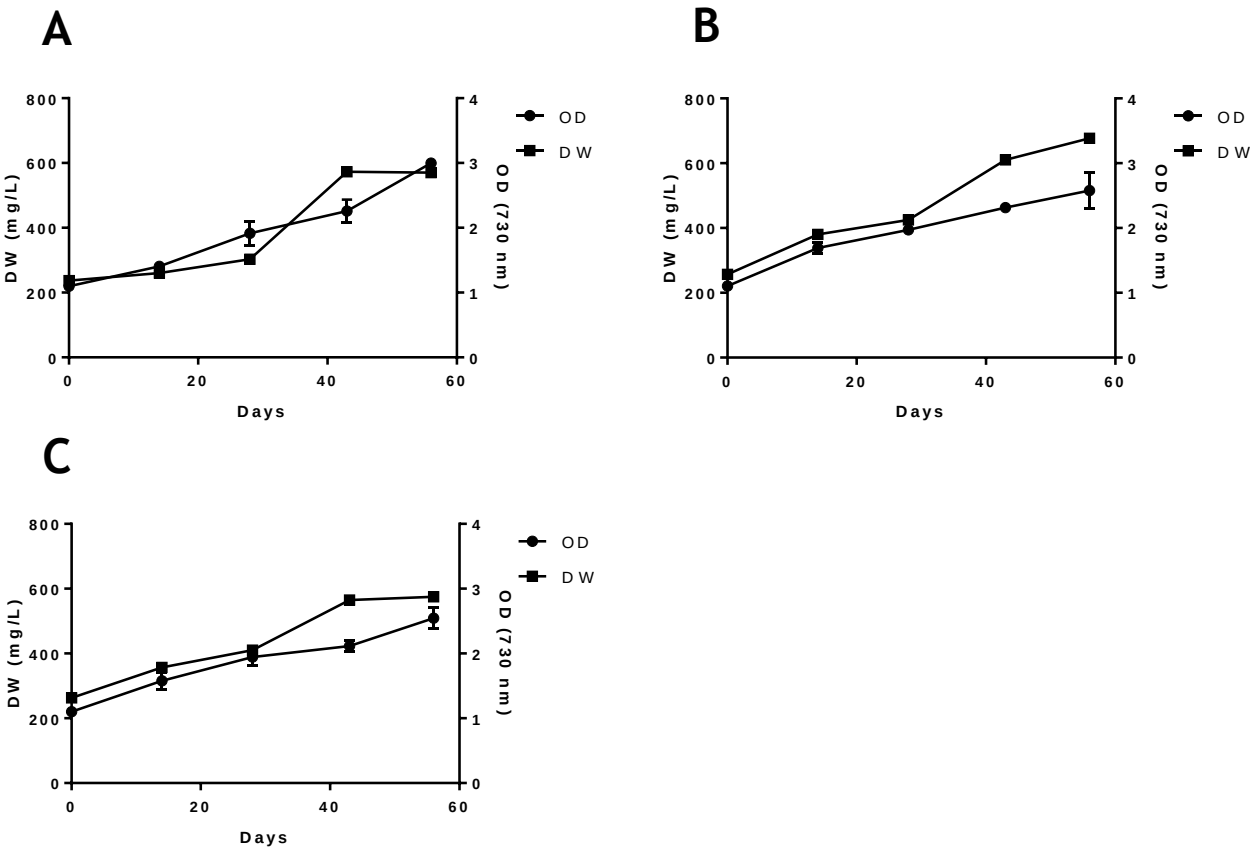

Fig. 20 - Growth of *Cyanothece* sp. CCY 0110 expressed as OD_{730nm} and mg of DW per L of (A) ANSIII, (B) ASNIII with sea water and (C) NutriBloom plus with sea water culture media. Cultures were grown in 500 mL flasks, at 25 ºC, a 16 h light (30 µmol photon m^{-2} s^{-1})/8 h dark regimen. The values are means ± standard deviations (n =3).

Therefore, as example, it is possible to stipulate that an OD_{730nm} of 3 corresponds to a DW value of 570 mg/L of culture grown in ASNIII medium (fig. 20(A)), an OD_{730nm} of 2.6

corresponds to a DW value of 676.7 mg/L of culture grown in ASNIII with sea water medium (fig. 20(B)) and an OD_{730nm} of 2.6 corresponds to a DW value of 537 mg/L of culture grown in NutriBloom Plus with sea water medium (fig. 20(C)). Specific growth rates (using OD_{730nm}) of cultures grown using different media were also calculated for growth evaluation. Achieved specific growth rates for ASNIII, ASNIII with sea water and NutriBloom Plus with sea water media were $\mu=0.0078\ day^{-1}$, $\mu=0.0066\ day^{-1}$ and $\mu=0.0065\ day^{-1}$, respectively.

To determine if the carbohydrate production was affected by the change of culture media, CHT and RPS contents were measured. Fig. 21 strongly suggests that CHT and RPS contents per L of culture followed the same pattern regarding all types of culture media, having an increase of about 2- to 3-fold from the beginning until the end of cultivation period. In addition, the analysis of the percentage of RPS present in the culture throughout the growth curve suggests a constant rate of these polysaccharides in cultures grown in all types of media, representing 80.6 ± 4.8% of CHT using ASNIII medium, 81.9 ± 6.1% using ASNIII with sea water medium and 83.1 ± 6.9% using NutriBloom Plus with sea water medium.

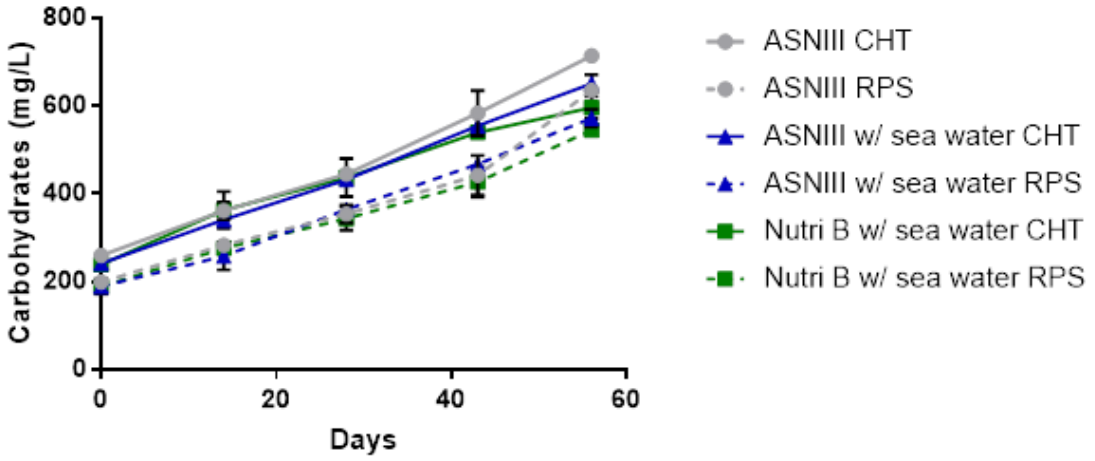

Fig. 21 - Total carbohydrates (CHT) and RPS content expressed as mg per L of ASNIII, ASNIII with sea water and NutriBloom plus with sea water culture media (mg/L). Cultures were grown in 500 mL flasks, at 25 ºC, a 16 h light (30 µmol photon m^{-2} s^{-1})/8 h dark regimen. The values are means ± standard deviations (n = 3).

The amount of carbohydrates produced by *Cyanothece* cultures grown with different media was also normalized to DW concentration in order to evaluate the production of carbohydrates at the cell level. As it can be seen in fig. 22, the CHT and RPS contents (mg) per mg of DW were similar throughout the cultivation period regarding all types of culture media, showing a constant rate of carbohydrate production over time independently of the culture media tested.

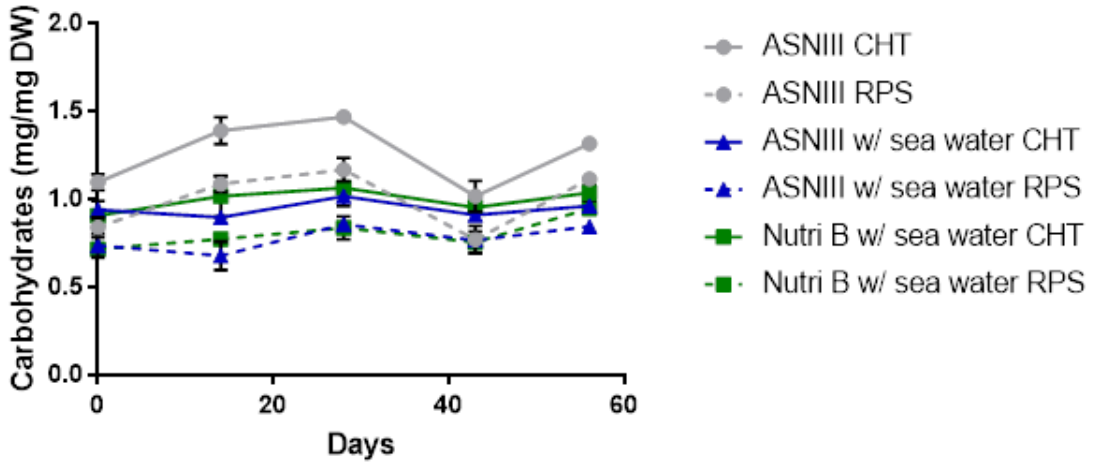

Fig. 22 - Total carbohydrates (CHT) and RPS content, expressed as mg per mg of DW (mg/mg DW), of cultures grown in ASNIII, ASNIII with sea water and NutriBloom plus with sea water culture media. Cultures were grown in 500 mL flasks, at 25 ºC, a 16 h light (30 µmol photon m^{-2} s^{-1})/8 h dark regimen. The values are means ± standard deviations (n = 3).

5.2- RPS coating development

5.2-1. Surface characterization

Along with RPS-polymer production, isolation and purification processes, the goal was to optimize the application of this polymer as an anti-adhesive coating capable of hindering bacterial attachment, and therefore preventing biofilm formation on indwelling devices, such as polyurethane catheters. Different approaches for coating development were tested comparing lab-based linkage processes to more industrialized methods used in coating fabrication. Surface characterization of unmodified and modified polyurethane (PU) surfaces through the different strategies was performed using various methods, such as optical contact angle measurements (OCA), scanning electron microscopy (SEM), x-ray photoelectron microscopy (XPS) and attenuated total reflection – Fourier-transform infrared spectroscopy (ATR-FTIR). Additionally, an Alcian blue staining of RPS-coated surfaces was also performed.

5.2-1.1. Optical contact angle (OCA)

Contact angle measurements can be used as an indication of the degree of surface modification efficiency, particularly when the modification can be related to an increase/decrease of surfaces wettability. As mentioned before, two different OCA measurements were used: sessile drop and captive bubble, depending on the samples and on the facility where experiments were conducted (fig. 23).

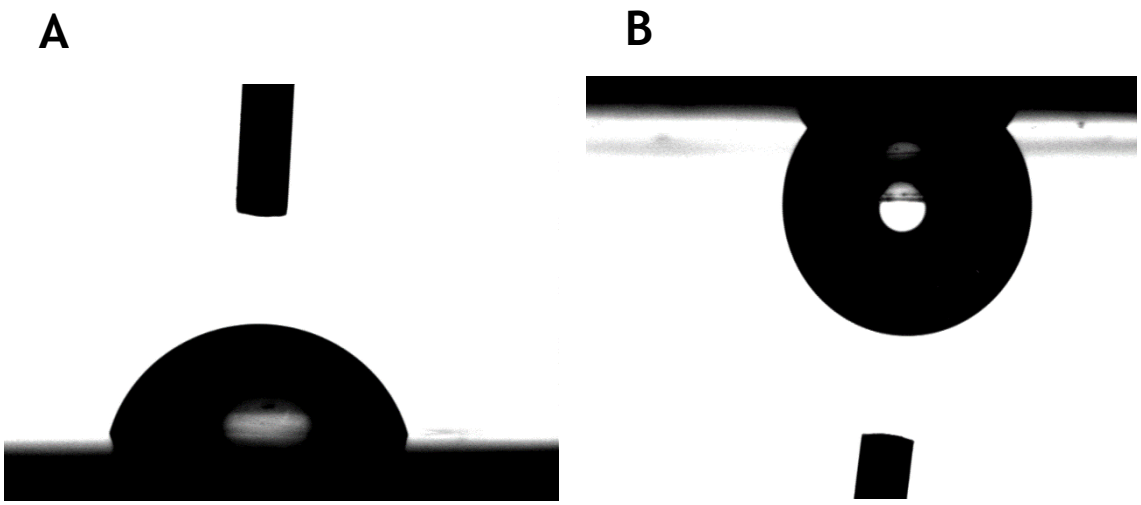

Fig. 23 - Example of (A) sessile drop and (B) captive bubble droplet/bubble profile of an uncoated polyurethane (PU) surface.

i) Study and optimization of coating linkage to substrate strategies

The optimization of pDA layer application and consequent coating deposition was performed using captive bubble measurements of two different pDA incubation periods (18 and 24 h) (fig. 24). Uncoated PU films presented a water contact angle of 50.4 ± 1.8 °, which was significantly diminished after the application of pDA layer to 27.9 ± 1.8 ° (18 h) and 30.9 ± 3.8 ° (24 h). The samples after RPS application revealed an even more hydrophilic behaviour, 16.1 ± 1.2 ° (18 h) and 16.4 ± 1.6 °(24 h) respectively, suggesting the success of RPS-based coating production. No statistical difference was observed between the two pDA incubation periods. Therefore, the 18 h incubation period was selected for further coating production and performance evaluation.

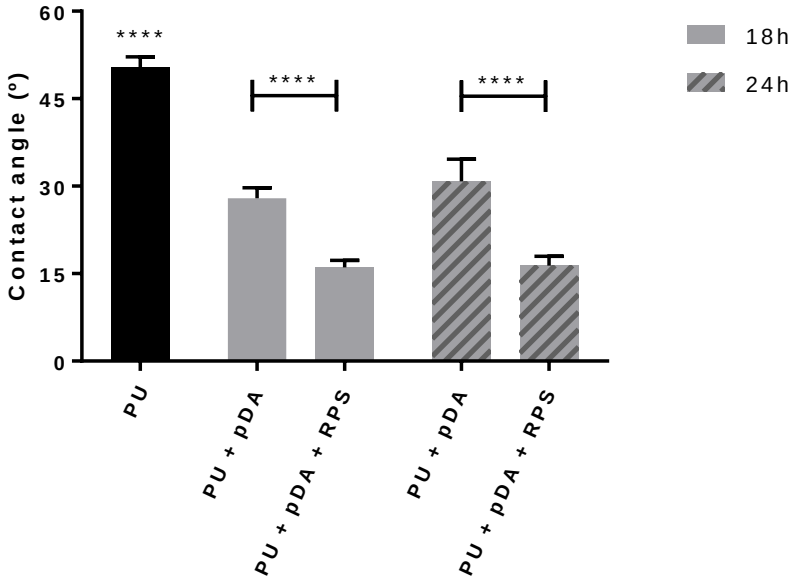

Fig. 24 - OCA captive Bubble measurements (Tangent curve-fitting) of original PU, PU+pDA and PU+pDA+RPS using two different incubation periods (18 h and 24 h). The values are means ± standard deviations (n=3). Statistically significant differences were calculated through ANOVA and are indicated with: **** p value ≤ 0.0001.

Regarding PU films activation through plasma pre-treatments, optimization was performed testing different combinations of applied power (kW) and frequency of motor rotation (Hz) (Table 2), and efficiency of the different methods was assessed by sessile drop technique (fig. 25). Uncoated PU presented a water contact angle of 70.4 ± 3 °, which was different to the previously obtained in the pDA layer deposition optimization through captive bubble method. This may be related to the different techniques applied to the measurement (captive bubble and sessile drop, respectively), and will be further discussed in the discussion chapter.

Table 2 - Different plasma parameters combinations of applied power (kW) and frequency of motor rotation (Hz).

Plasma parameters combinations	Applied power (kW)	Frequency (Hz)
P1	7.5	3.3
P2	11.3	3.3
P3	15.0	1.1

All tested activation combinations resulted in a decrease in contact angles comparing to uncoated PU. O_2-plasma activated surfaces exhibited contact angles ranging from 60.3 ±

2.4° and 60.4 ± 3 ° (when using P2 and P3 parameters, respectively) to 65.5 ± 2.4 ° (when using P1 parameters), while N_2-plasma activated surfaces exhibited contact angles ranging from 61.5 ± 0.5 ° and 61.3 ± 0.7 ° (when using P2 and P3 parameters, respectively) to 63.7 ± 0.5 ° (when using P1 parameters) (fig. 25(A)).

Although most of different parameters tested in each plasma activation technique led to significant contact angle decreases when compared to uncoated PU, the medium/high intensity P2/P3 parameters appeared to introduce a more pronounced effect of activation, exhibiting the lowest contact angles. As no significant difference was observed between P2 and P3, P2 parameters were selected for further study of O_2/N_2 plasma-treated surfaces and consequent coating application and performance evaluation. Moreover, no significant difference was observed between contact angles measured after O_2 or N_2 plasma treated PU surfaces suggesting that the efficiency of plasma surface activation was independent of the type of selected reactive gas. Regarding ozone activation, also a significant decrease on contact angle values was observed, when compared to untreated PU, exhibiting a contact angle of 59 ± 1 °.

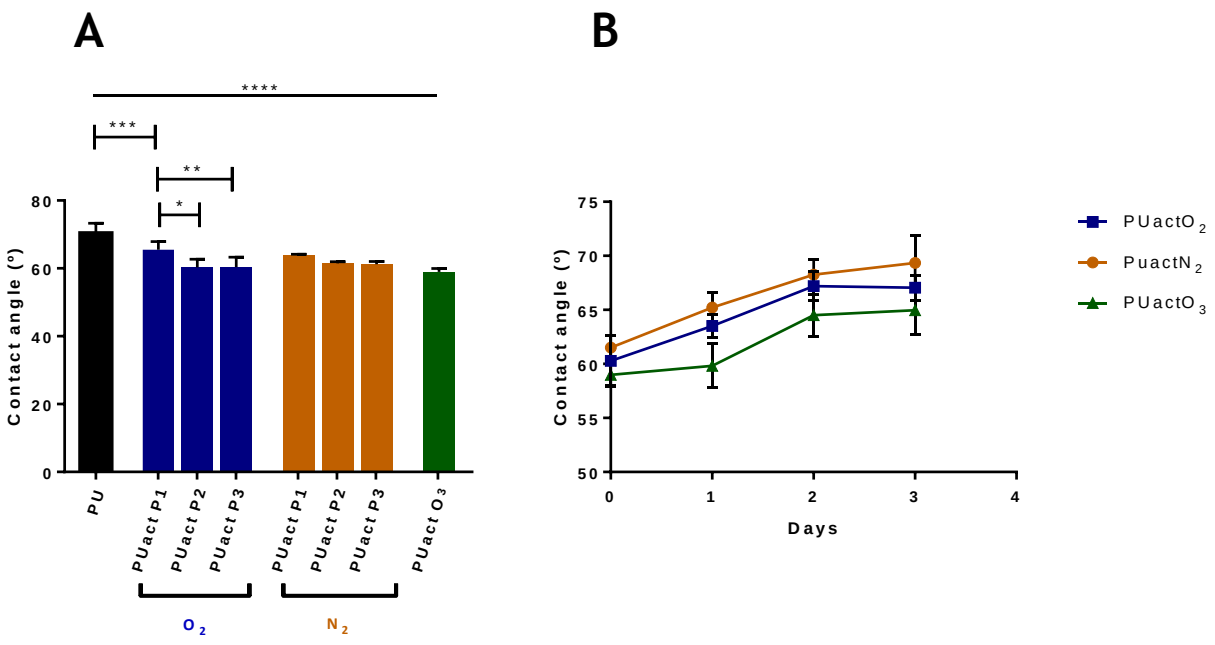

Fig. 25 - OCA sessile drop measurements (Young-Laplace curve-fitting) of: (A) PU, PUactO_2/N_2 using different parameters combinations and PUactO_3; (B) O_2/N_2 plasma and ozone treated surfaces throughout 3 days. The values are means ± standard deviations (6 measurements per sample). Statistically significant differences were calculated through ANOVA test and are indicated with: * p value ≤ 0.05; ** p value ≤ 0.01; *** p value ≤ 0.001; **** p value ≤ 0.0001.

Hydrophobic recovery and aging of plasma- and ozone-activated samples was evaluated by contact angle monitoring (sessile drop) during 3 days in order to monitor the loss of treatments effect, an important factor when considering storage purposes before coating application. As it can be seen in fig. 25 (B), there was an increase in contact angles throughout

the 3 days independently of the treatment type. O_2 plasma, N_2 plasma and ozone treated surfaces started with contact angles of 60.3 ± 2.4 °, 61.5 ± 0.5 ° and 59 ± 1.0 °, respectively, which have increased over the 3 days, reaching contact angle values close to the original PU films (67 ± 1.0 °, 69 ± 2.5 ° and 65 ± 2.3 °, respectively).

ii) Study and optimization of RPS coating application

After pre-treatments for improved coating linkage to substrate, surfaces were spin/immersion-coated with RPS solution.

Regarding samples obtained by spin-coating, an increase of hydrophilicity after coating process was observed, independently of the strategy used for coating linkage to substrate (fig. 26(A)). The lowest measured contact angles were recorded for pDA layer-related samples (16.4 ± 1.6 °), while O_2 and N_2-plasma-related surfaces exhibited similar lower contact angles values (18.7 ± 1.9 ° and 19.3 ± 1.6 °, respectively). Coatings produced through ozone pre-treatment also resulted in significant increase of wettability, showing contact angles of 24.7 ± 2.3 °. The overall results of OCA suggest that the spin-coating process was able to efficiently deposit RPS coating on all pre-treated surfaces when comparing to pre-treated and uncoated PU surfaces.

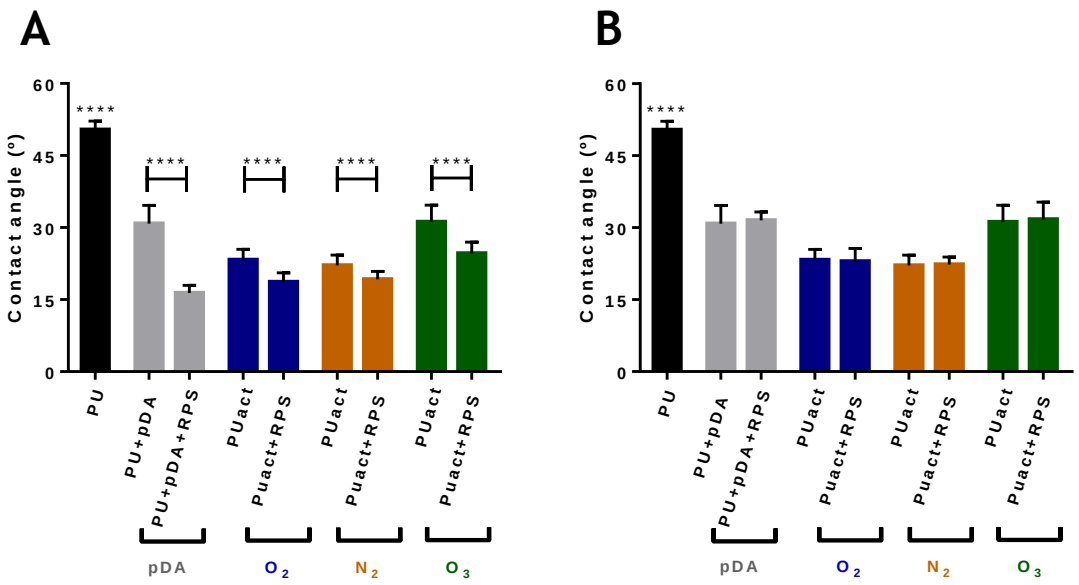

Fig. 26 - OCA captive bubble measurements (Tangent curve-fitting) of unmodified and modified surfaces through (A) spin-coating (3 assays) and (B) immersion-coating (1 assay). The values are means ± standard deviations (n=3). Statistically significant differences were calculated through ANOVA test and are indicated with: **** p value ≤ 0.0001.

activated surfaces through all the different linkage strategies using immersion-coating process did not display the same kind of angle reduction as the spin-coating process (fig. 26(B)). Measured angles did not exhibit significant contact angle reductions when compared to pre-treated surfaces, suggesting that the coating deposition was not being performed efficiently.

Spin-coating method was selected for subsequent coating production in order to do further surface characterization and performance evaluation.

5.2-1.2. Scanning electron microscopy (SEM)

Scanning electron microscopy (SEM) was used to obtain high-resolution three-dimensional surface images, offering information about surface topography modification after pDA, plasma and ozone activations, as well as, after coating application (fig. 27).

Regarding activated PU surfaces (fig. 27 (B, D, F, H)) different surface topographies were found depending on the applied activation technique (pDA layer, plasma and ozone treatments, respectively). pDA layer application on PU surfaces seemed to introduce a smoother topography to PU substrate (fig. 27(A)) while the surface activation through plasma and ozone treatments seemed to increase surface roughness (fig. 27(D, F, H)). Regarding N_2 plasma activation (fig. 27(F)), some holes of different sizes were observed throughout the PU modified surface that can also be observed on the related coated surfaces (fig. 27(G)). This was due to operational problems on plasma equipment during this particular surface activation procedure during samples preparation for SEM analysis.

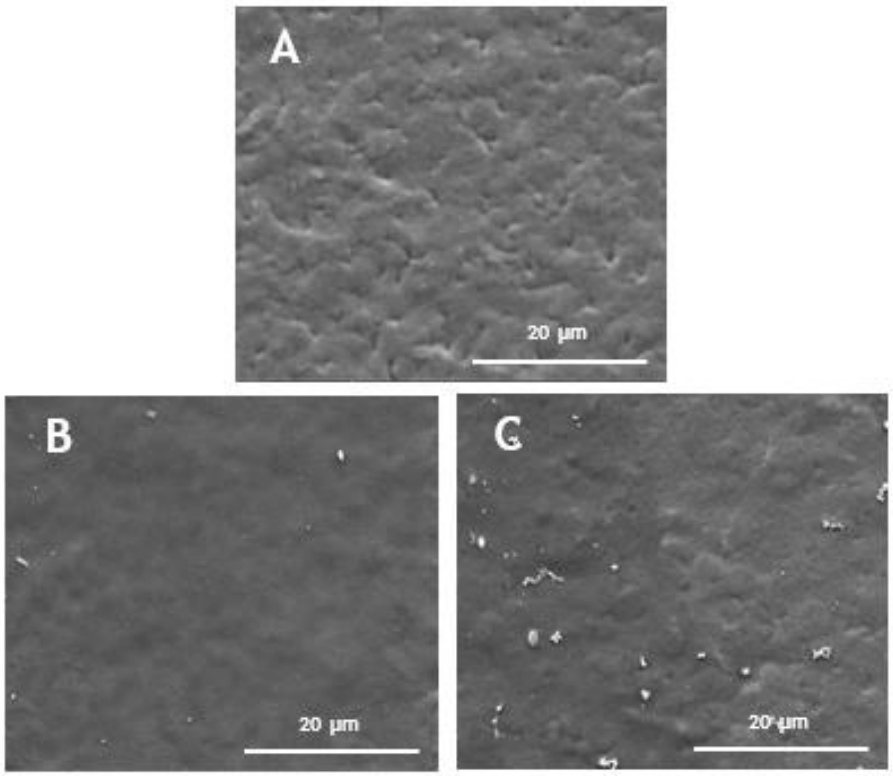

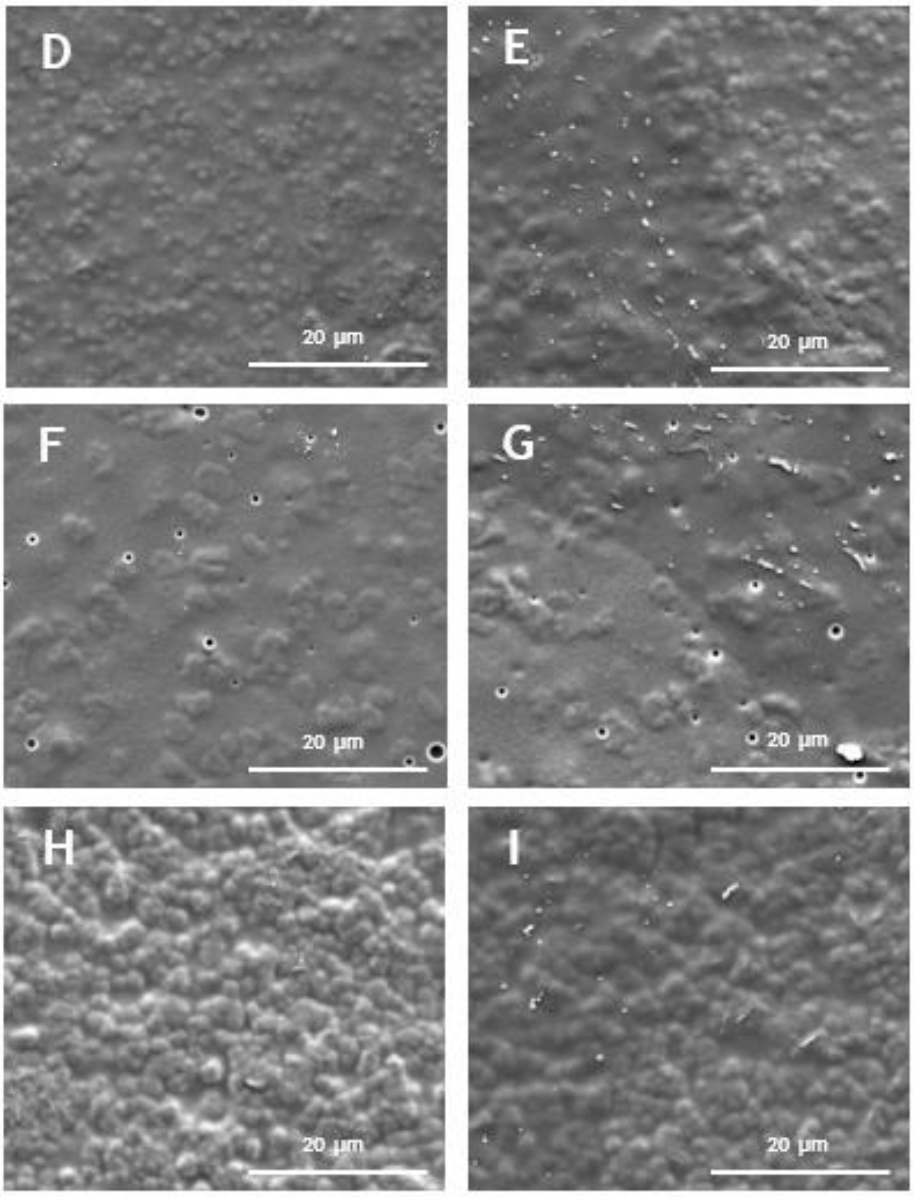

Fig. 27 - Scanning electron microscopy (SEM) micrographs (magnification of 5000x) of modified PU surface. (A) PU; (B) PU+pDA; (C) PU+pDA+RPS; (D) PUactO_2; (E) PUactO_2+RPS; (F) PUactN_2; (G) PUactN_2+RPS; (H) PUactO_3; (I) PUactO_3+RPS.

On micrographs regarding RPS-coated samples via O_2/N_2-plasma and ozone pre-treatments (fig 27(E, G, I)), it was observed a smoother surface topography after spin-coating process, suggesting RPS deposition. However, polymer deposition appeared to have a heterogeneous distribution, given by the differences in the micrographs brightness, suggesting differences in topography. This could be due to different coating densities throughout surfaces: darker regions - increased coating density and brighter regions - decreased coating density. EDS analysis in both regions did not show differences in composition. RPS-coated surfaces via pDA layer application seemed to have the most homogeneous and uniform coating deposition (fig. 27(C)).

5.2-1.3.X-ray photoelectron spectroscopy (XPS)

Relative atomic composition of unmodified and modified surfaces was determined using XPS analysis. Fig. 28 represents the survey spectra obtained from unmodified PU surface. This spectrum revealed that the main components present on PU surfaces were C (81.6%) and O (16.4%), and in a lower percentage N (2%).

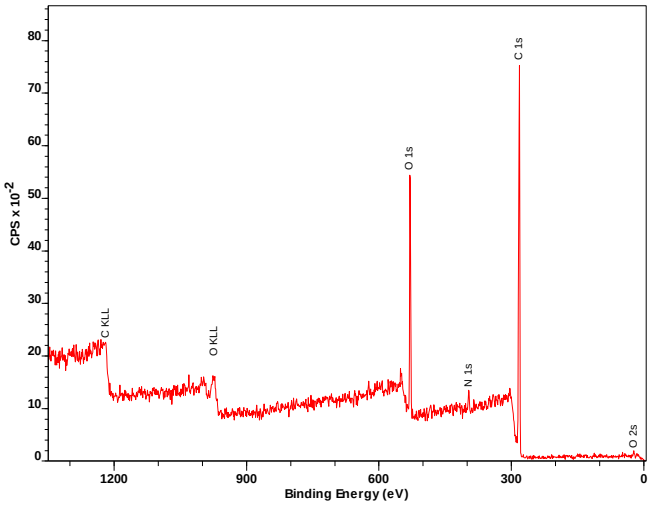

Fig. 28 - Representation of survey spectra of unmodified PU surfaces expressing O, N and C elements on its elemental atomic composition.

Fig. 29 shows the relative atomic % of the elements present on pre-treated and RPS coated surfaces. C/O ratios of polydopamine, O_2-plasma, N_2-plasma and ozone pre-treated surfaces, calculated from XPS atomic composition analysis, were 5, 5, 4 and 7, respectively. Additionally, PU surfaces with the pDA layer expressed a significant increase in the percentage of N (C/N PU= 40.8; C/N PU+pDA= 16.3).

Atomic composition of coated PU revealed that the main components present on RPS coating were C and O. Coatings produced through pDA strategy expressed a C/O ratio of 3, while plasma and ozone treatments achieved C/O ratios of 4 and 5, respectively. The different coating production strategies presented an overall decrease on C/O ratios when compared to unmodified or pre-treated PU. Moreover, less represented elements also appeared on coated surfaces - sulphur (S) on coatings produced via pDA layer (fig. 29 (A)) and nitrogen (N) on coatings produced via plasma and ozone activations (fig. 29 (B, C and D)).

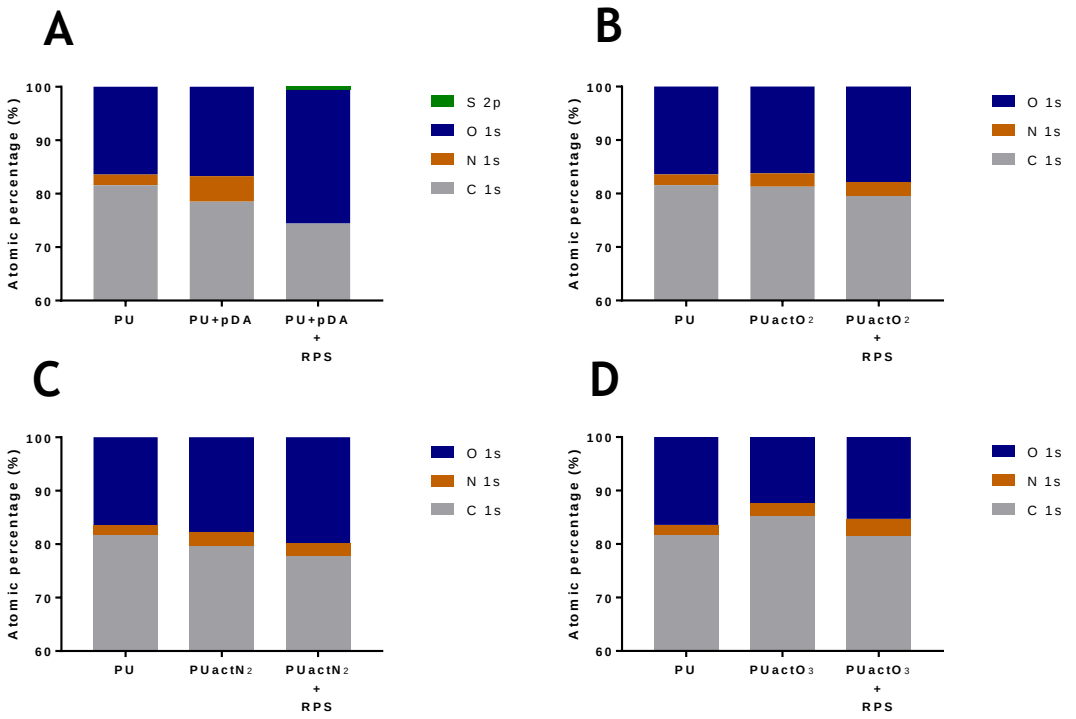

Fig. 29 - Representation of elemental atomic composition (%) of pre-treated and coated PU surfaces through (A) pDA layer application strategy, (B) O_2-plasma surface activation strategy, (C) N_2-plasma surface activation strategy and (D) ozone surface activation strategy.

5.2-1.4. Fourier-transform infrared spectroscopy in attenuated total reflectance mode (ATR-FTIR)

ATR-FTIR was performed to evaluate modification in surface chemical bonds on the different RPS coated surfaces (fig. 30).

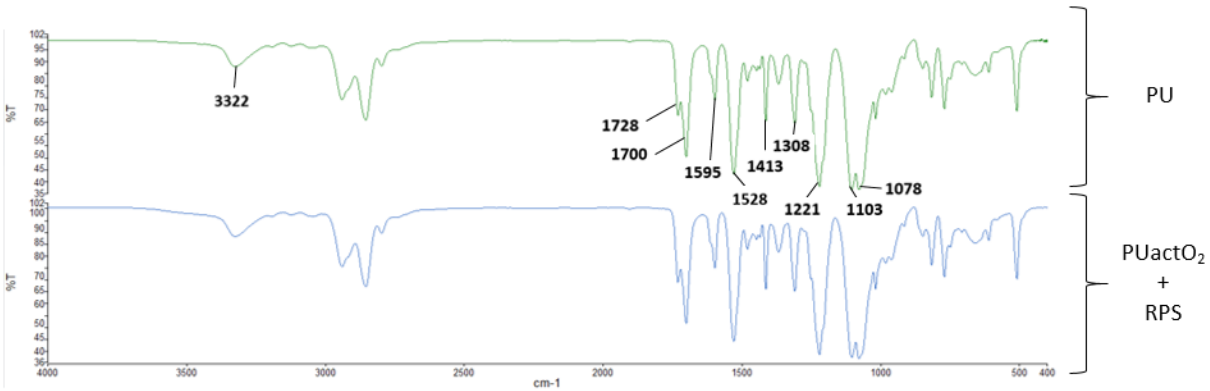

Fig. 30 - Representation of an example of ATR-FTIR spectra of PU and $PUactO_2$+RPS.

ATR-FTIR spectra of PU films demonstrated PU characteristic absorption bands, namely the absorption bands at 1595 cm^{-1} and 1413 cm^{-1} from benzene ring and at 1528 cm^{-1} from N-H and C-N from the urethane group. Absorption bands between 3300-3500 cm^{-1} indicate primary amine groups, 1690-1730 cm^{-1} indicate C=O groups and 2800-3000 cm^{-1} indicate CH_3 groups [86], [130]. However, no significant differences could be observed when comparing spectra of uncoated and coated PU surfaces.

5.2-1.5. Alcian Blue (AB) staining of RPS-coated surfaces

In order to clarify the presence of the coating throughout each of pre-activated PU surfaces, a staining using Alcian Blue dye was performed.

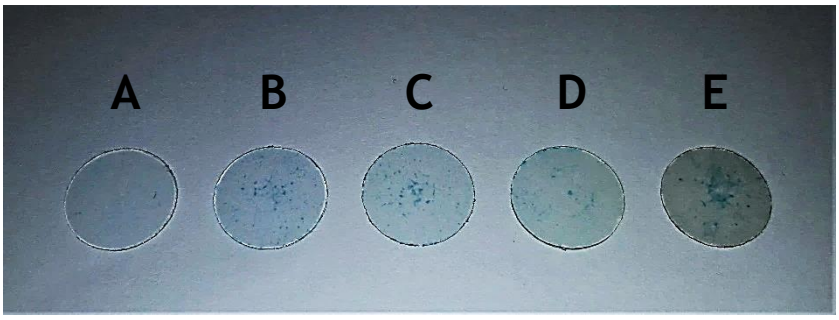

Fig. 31 - Alcian Blue staining of (A) uncoated PU surface; (B) PUactO_2+RPS; (C) PUactN_2+RPS; (D) PUactO_3+RPS; (E) PU+pDA+RPS.

As it can be seen in fig. 31, contrary to original PU surface (control), all of coated surfaces through the different coating production strategies, turned into a blueish colour after staining procedure, suggesting the polysaccharide-based coating presence on top of PU pre-treated surfaces. Moreover, the Alcian Blue stain was spread through the entire coated surface, although with some differences in intensity in some regions, suggesting possible thickness differences.

5.2-2. RPS coating degradability evaluation

RPS coating degradability evaluation was performed by an accelerated degradation assay adapted from ISO10993-13 (2009) protocol, which included high temperature (45 ºC) and exposure to different pH (pH 5 & pH 7.4). After the 7 days challenge samples were evaluated by OCA. Results are presented in fig. 32.

When compared to freshly prepared RPS coated surfaces (Day 0), samples that were exposed to 45 °C for 7 days (Day 7 45 °C) presented similar water contact angles, independently of coating production strategy. Additionally, no differences were observed between Day 0 and after 1 h incubation on the defined pH buffers (5 & 7.4). Moreover, the exposure of different

RPS coated surfaces to the combination of accelerated degradation conditions (T & pH) did not result in significant wettability changes in comparison to freshly prepared samples, with the exception of PU coated surfaces via pDA linkage (fig. 32(A)). In this particular case, the combination of 45 °C with pH 5 resulted on a 2 ° increase of the water contact angle, when compared to freshly prepared coated surfaces (Day 0).

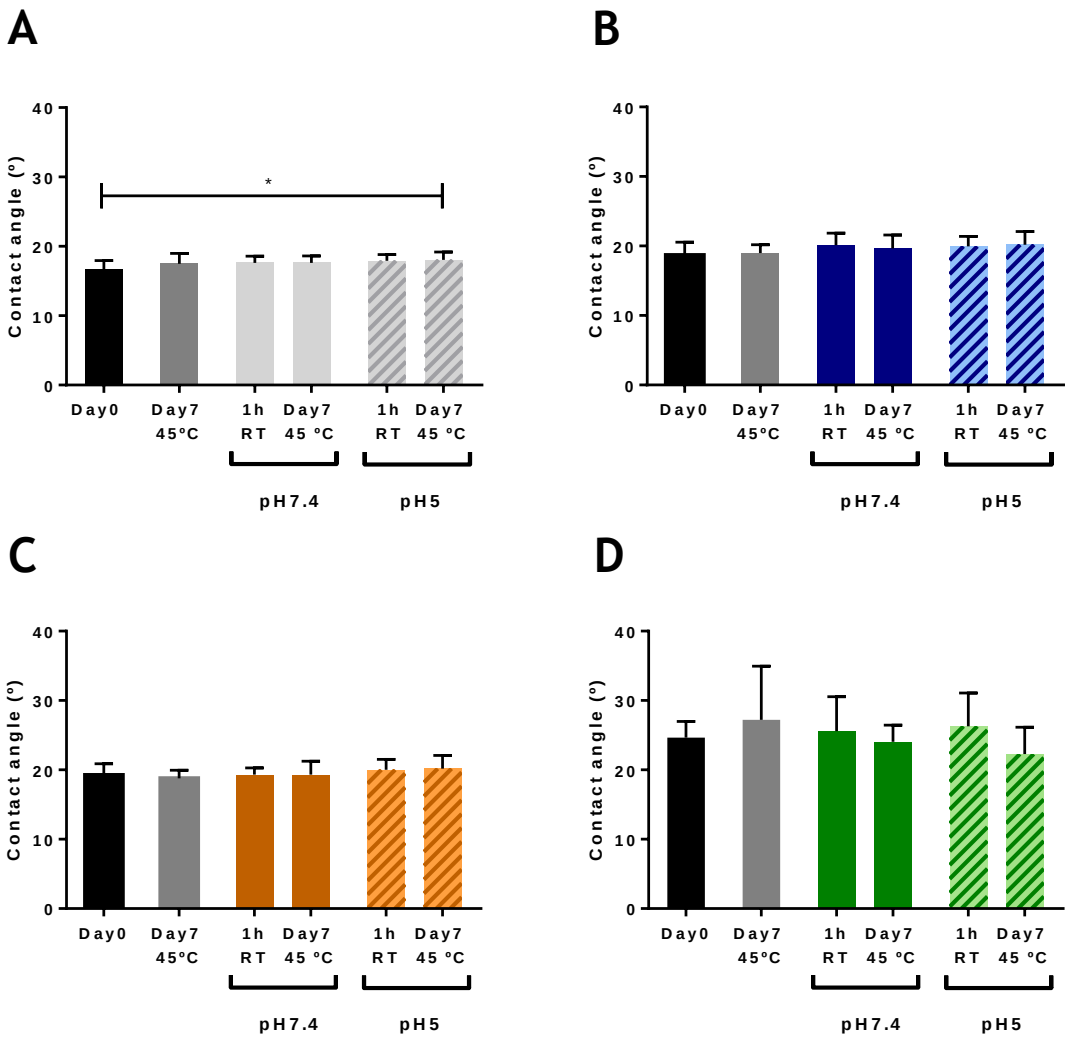

Fig. 32 - OCA Captive bubble measurements (Tangent curve-fitting) of spin-coated surfaces via (A) pDA layer application, (B) O_2 plasma treatment, (C) N_2 plasma treatment and (D) ozone treatment exposed to accelerated degradation conditions: Freshly prepared RPS coating (RPS control) - **Day0**; RPS coating incubated 7 days at 45 °C - **Day7 45 °C**; RPS coating incubated 1h at RT in PBS (pH 7.4) - **1h RT (pH7.4)**; RPS coating incubated 7 days at 45 °C in PBS (pH7.4) - **Day7 45 °C (pH7.4)**; RPS coating incubated 1h at RT in acetate buffer (pH 5) - **1h RT (pH5)**; RPS coating incubated 7 days at 45 °C in in acetate buffer (pH5) - **Day7 45 °C (pH5)**; The values are means ± standard deviations (n = 3). Statistically significant differences were calculated through ANOVA test and are indicated with: * p value ≤ 0.05.

5.2-3. RPS coating anti-adhesive performance evaluation

Coated PU surfaces through the different strategies were subjected to bacterial anti-adhesive assays in order to evaluate the efficiency of the coatings regarding bacterial adhesion prevention.

As it can be seen in fig. 33, coatings produced via pDA layer linkage seemed to have a high impact on the adhesion of different bacteria to the surfaces, either in the absence or presence of plasma proteins. When testing *S. aureus* (fig. 33(A)), this type of coating showed a 93.5% reduction on adhered bacteria in the absence of plasma and 55% reduction in the presence of plasma. Regarding *S. epidermidis* (fig. 33(B)), an even more dramatic adherence decrease was observed when comparing to uncoated PU, either in the presence (97.2%) or absence (99%) of plasma proteins. Contrary to *S. aureus*, *S. epidermidis* seemed to adhere less to surfaces in the presence of blood plasma. *E. coli* adherence to this type of substrates (fig. 33(C) in the absence of plasma proteins, was also significantly reduced (95.3%) when compared to uncoated PU surfaces.

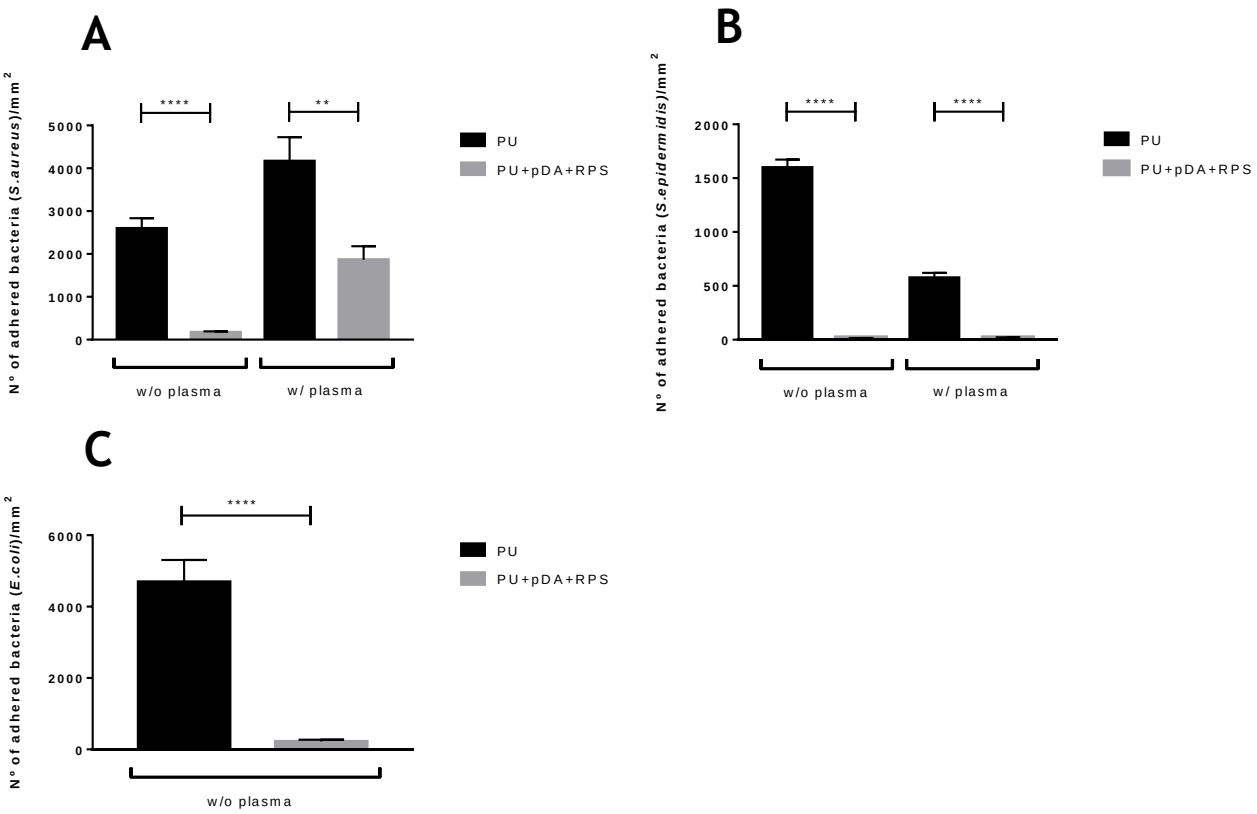

Fig. 33 - Total bacterial adherence expressed as number of adhered bacteria per mm^2 on PU and PU+pDA+RPS surfaces using (A) *S. aureus* and (B) *S. epidermidis* in the presence or absence of blood plasma (1%, v/v), and (C) *E. coli* in the absence of blood plasma. The values are means ± standard deviations (n = 12, 1 assay). Statistically significant differences were calculated through Kruskal-Wallis test (A & B) or Paired t-test (C) and are indicated with: ** p value ≤ 0.01; **** p value ≤ 0.0001.

RPS coated samples obtained by the industrialized activation methods were also tested for bacterial anti-adhesive performance (fig. 34).

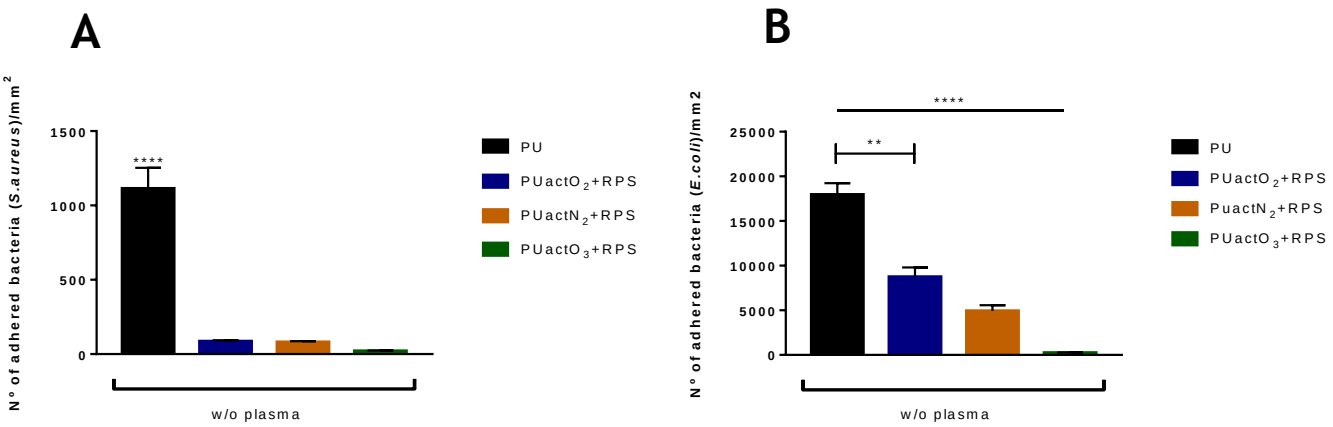

Fig. 34 - Total bacterial adherence in the absence of blood plasma expressed as number of adhered bacteria per mm^2 on PU, $PUactO_2$+RPS, $PUactN_2$+RPS and $PUactO_3$+RPS surfaces using (A) *S. aureus* and (B) *E. coli*. The values are means ± standard deviations (n = 6). Statistically significant differences were calculated through Kruskal-Wallis test and are indicated with: ** p value ≤ 0.01; **** p value ≤ 0.0001.

When using *S. aureus* as bacterial model (fig. 34(A)), RPS coated surfaces through O_2 and N_2-plasma treatment had a significant impact on bacterial adhesion prevention reaching a similar adherence reduction of 93%, in comparison to uncoated PU surfaces. RPS-coated surfaces via ozone treatment also greatly affected *S. aureus* adhesion, promoting a 98% reduction on bacterial adherence. When using the gram-negative *E. coli,* the impact of RPS coated surfaces via O_2 plasma treatment seemed to be more moderate on bacterial adhesion rates showing a 51% decrease (fig. 34(B)). Nevertheless, coatings produced through N_2 plasma activation resulted in a more pronounced decrease of *E. coli* affinity towards these surfaces, showing a 73% adherence reduction, while coated surfaces through ozone pre-treatment displayed a 99% adhesion reduction rate when compared to unmodified PU surfaces.

Chapter 6

Discussion

6.1- Evaluation of culture scale-up and the use of different media with reduced cost on *Cyanothece* sp. CCY 0110 growth and RPS production

Here, a 5-fold scale-up of *Cyanothece* sp. CCY 0110 culture was established using 5 L bioreactors. The main goal was to evaluate the influence of the scaling-up procedure (testing modifications on bioreactor geometry and increase of culture volume) on growth and carbohydrates production, maintaining previously described growth conditions (light, aeration, temperature, stirring – see section 4.1-1.).

Different parameters were used for growth evaluation. Optical density (OD) at 730 nm is routinely used to monitor the growth of unicellular cyanobacterial cultures [83]. Evaluation of dry weight (DW) parameter is important not only to evaluate cell density but also to allow normalization of the data. Specific growth rate is also considered to be a good indicator of growth performance [84].

First of all, 5-fold scale-up of *Cyanothece* culture exhibited a linear and slow growth without a clear exponential phase. This is a common characteristic for strains that produce large amounts of structured extracellular polysaccharides [87]. It has been hypothesised that this type of growth curve may be related to the substantial amount of energy necessary for the production of EPS [87], [88]. In fact, the growth values presented here have shown a quite similar pattern when compared to *Cyanothece* grown in 1 L bioreactors [68]. However, there was a decrease on the growth rate, once the cultures grown in 1 L bioreactors achieved a specific growth rate of μ=0.02 (day^{-1}). Several factors can justify the decrease in specific growth rate after the culture scale-up. The change of bioreactor geometry can influence the light exposure, stirring and aeration of the culture, therefore hampering the light penetration/distribution, which was proven to be the key parameter in cell growth regarding this strain [68]. All these results suggested that, 5-fold scale-up did not negatively affect

Cyanothece growth. However, there is still necessary to perform some optimization of the culture conditions (light intensity, aeration and/or stirring) aiming at improving the overall growth rate.

In order to evaluate the influence of the scale-up on *Cyanothece* carbohydrates production, total carbohydrates (intracellular and extracellular carbohydrates including RPS) and RPS contents were measured by the phenol-sulphuric acid method. Although this technique is well established [85], it is important to take into consideration that may be an underestimation since not all of amino sugars react in this method [89]. Total carbohydrates and RPS concentrations followed the same pattern and were in the range of values previously reported for cultures grown in 1 L bioreactors, although it seems that there was an overall decrease on the carbohydrates production when comparing to 1 L cultures grown with similar culture conditions [68]. Nevertheless, the data presented here confirmed the high RPS production rate of this particular *Cyanothece* strain, representing 78 ± 3% of total carbohydrates. This is important since RPS are easier to recover compared to EPS that remain attached to the cell surface, conferring an advantage to its potential use in biotechnological and industrial applications. The increase in the amount of carbohydrates throughout the growth curve seen here, can be mainly a result of the progressive accumulation of RPS in the culture medium, with the lower amount belonging to the cell wall or intracellular carbohydrates [61]. Generally, the amount of carbohydrates produced per DW (and consequently per cell) did not vary significantly when comparing the beginning and the end of cultivation period. These results strongly suggest that carbohydrate production was not specific to a determined stage of growth and that the variation in the amount of carbohydrates present in the culture was mainly related to the number of cells, rather than to the amount of carbohydrates produced by each cell, as previously observed [68].

The lower amount of produced and isolated RPS achieved during this work (1.1 g/L), in comparison with the isolated RPS from *Cyanothece* cultures grown in 1 L bioreactor (1.8 g/L) [68], suggested a possible impact of scaling up modifications on polymer production. However, it should be taken in consideration that i) the polymer purification process used here was optimized (two steps of increased centrifugation speed and precipitation with 99% ethanol) and ii) the increased volume of culture demanded a more complex handling of extraction procedures. All of these facts can justify some loss on the quantity of isolated polymer. Considering other strains of *Cyanothece*, previous studies have reported higher amounts of produced and isolated RPS (2.36 g/L when using *Cyanothece* CA 3 [59]), while lower amounts were reported for *Nostoc calcicola* RDU-3 and *Anabaena* WSAF [60].

As soon as the culture conditions are optimized in order to increase the cyanobacterial RPS production, it is necessary to develop economic, effective and environmentally friendly process to extract high yield of RPS for industrial applications. These extraction processes are also necessary to obtain polysaccharides with a high purity degree. RPS solubilised in culture medium are usually separated from the cells using centrifugation or microfiltration [90]. Thereafter, the soluble fraction (named supernatant or filtrate) is precipitated using absolute

alcohols, such as methanol, ethanol (used here) or isopropanol (2–3 volumes of alcohol for one volume of supernatant) [90], [91]. The polarity of alcohol and the temperature of precipitation (between −20 °C and 20 °C) can have an impact on the RPS yield but also on the co-precipitation of impurities. This method allows the selective concentration of RPS and has several advantages such as the possibility to recycle alcohols by distillation and to treat highly viscous solutions [90]. Marine cyanobacteria are often contaminated by salts, which can co-precipitate with the polysaccharides. Introducing a dialysis step prior to centrifugation ensures the removal of this type of contamination [91]. Nevertheless, the search for improved methods regarding RPS isolation and purification will allow improved yields and its cost-effective production, factors extremely important for consequent industrial application, namely as a coating.

In certain cases, the medium is estimated at about 80% of the cyanobacterial culture establishment costs [82] and can, therefore, make the process economically unfeasible. Cultivation of cyanobacteria can be conducted on a diversity of culture media (depending on the requirements of each strain) that usually contain the same nutritional elements but with slightly differing amounts [90]. They include nitrogen (N), phosphorous (P) and sulphate (S) sources, trace-metal (such as cooper, manganese and iron) and vitamins (generally cobalamin, biotin and thiamine-HCl). Apart from a few exceptions, there has been no study performed to simplify these media and to verify which nutrient is really required by the cells for growth and EPS production. Attention has only been paid on the three main nutrients (N, P and S), and especially on the impact of the lack of these nutrients on polysaccharides production. Nutrient limitation is a classical strategy for accumulation of targeted EPS. However, cell growth generally declines under those conditions [92]. There have been reported some successful strategies regarding the cost reduction of different media, such as modifications on the used reagents (modifications on nitrate nitrogen? source for example), or on the selected solvent for their dissolution (fresh/sea water) [93], [94]. ASNIII is a synthetic sea water medium that has proven to be adequate for sustainable *Cyanothece* growth [68], [81]. However, due to the quantities and types of reagents used on the preparation of this particular synthetic medium, the translation to an industrial context can become quite expensive in comparison to other minimal media. The reduction of media cost without compromising *Cyanothece* growth and carbohydrates production is extremely important when considering the RPS-based coating production in an industrial context. Here, two different reduced costs media were tested: ASNIII with sea water (ASNIII medium reagents with the exception of sodium chloride and type II water that is substituted by sea water) and NutriBloom Plus with sea water (1% (v/v) of commercial culture medium for cyanobacteria and microalgae cultivation enriched with vitamins in sea water). The use of a natural and abundant resource such as sea water, without the need of using high quantities of expensive sodium chloride and not so abundant fresh type II water is of great interest since it can contribute significantly for the media costs reduction. Additionally, a culture medium available in the market that has been already optimized for the growth of cyanobacterial strains at minimal costs is probably a good option for lowering media-

related costs. In this part of the work, the main goal was to evaluate the influence of above-mentioned media on *Cyanothece* growth and carbohydrate production, using already tested and validated ASNIII medium as a control.

Results shown here regarding growth evaluation by monitoring OD, DW and specific growth rate parameters did not reveal any noteworthy differences between cultures grown in different media, which indicated that these can be adequate for successful growth of *Cyanothece*. Carbohydrates production, in particular RPS, also did not seem to be affected by the culture media tested. Moreover, the values of total carbohydrates and RPS content (mg) per mg of DW were similar throughout the growth curve regarding all culture media, suggesting a constant rate of carbohydrate production per each cell independently of the type of medium used. Here, it was demonstrated the possibility of reducing medium cost in a successful way by the use of sea water and/or commercial medium. However, it should be considered that further studies are needed in order to achieve the highest rates of RPS production using the lowest cost medium possible.

6.2- RPS coating development, characterization and evaluation

After *Cyanothece*-derived RPS production scale-up, the goal was to develop an anti-adhesive coating based on this polymer, capable of preventing the adhesion of bacteria prevalent in catheter-associated infections.

For the improvement of coating linkage to the substrate (medical grade polyurethane (PU)), surfaces were exposed to different pre-treatment processes, namely the application of a layer of polydopamine and O_2/N_2-plasma or ozone surface activations. All of these processes have been proven to introduce radicals and/or functional groups that can serve as anchors for RPS coating improved linkage after its deposition [41], [46], [95]. pDA is a bio-inspired polymer (i.e. bio-glue) that deposits non-selectively from solution onto virtually any solid surface [44]. Additionally, pDA exhibits numerous celebrated properties including easy-to-implement, strong binding forces to different substrate surfaces, excellent biocompatibility and versatile post-functionalization accessibility [33]. Surface modifications using this molecule by just doing a simple immersion-coating process are able to be performed with greater ease and be applied to many types of material with complex shapes and multiple uses [45]. Plasma and ozone pre-treatments were chosen due to its easier translation to industrial settings. This is truly important when considering possible future industrial RPS coating application on catheters. Plasma surface modification has several advantages that makes this technology an excellent candidate for polymeric materials pre-treatment. It does not require hazardous solvents and does not affect bulk properties [96]. Nevertheless, usually plasma processes are limited to the treatment of flat and simple shaped materials. Surface oxidation through ozone exposure is also one of the most widely applied methods in polymer industries to improve surfaces

properties. Despite the fact that this type of surface treatment has been shown to degrade surfaces in some occasions, it also does not require hazardous solvents and can be applied to complex shaped materials [41]. Additionally, ozone exposure can be coupled to UV-light that have shown to enhance surface chemistry alterations [42].

The overall objective was to evaluate and understand which was the most promising strategy that could efficiently produce RPS coating on PU surfaces, taking into account not only the surface modification processes performance but also the costs and scalability of the selected processes.

Surface characterization of uncoated and coated PU was performed through different techniques: optical contact angle (OCA) measurements, scanning electron microscopy (SEM), x-ray photoelectron spectroscopy (XPS), Fourier-transform infrared spectroscopy in attenuated total reflectance mode (ATR-FTIR) and Alcian blue staining. The impact of the information obtained by each technique in the overall assessment of the coating production varied. Indeed, ATR-FTIR did not help to clarify the coating establishment, as its analysis depth did not allow to assess the presence of surface modification in thin coatings, as the ones described herein. Regarding OCA surface characterization, two different measurement techniques were used: sessile drop and captive bubble method, depending on the expectable wettability of the sample surface. Good agreement has been observed between sessile drop and captive bubble contact angles on clean smooth polymeric surfaces [97], but not in textured material [22]. In this work some differences on measured angles were found when using both techniques. This may be related to the different environments (air and water) where the angles were measured that may influence on droplet/bubble profiles when in contact with substrate [73]. In addition, different volumes of droplet/bubble were used in each technique that could also have influenced measured angles [98]. Nevertheless, contact angle measurements using both methods were able to distinguish between uncoated, pre-treated and coated PU surfaces. Regarding to XPS analysis, surface modifications where compared to the initial relative atomic composition of PU surfaces that have expressed no other elements than C, O and N, suggesting that there was no contamination. Additionally, the relative atomic composition of C, O and N elements obtained here was similar to previously reported on other studies using the same type of PU [128].

Starting with polydopamine, this strategy is known for allowing good linkage to the substrate, depending on the substrate, concentration of dopamine and time of incubation. These parameters are directly associated with the thickness of the layer and its stability [46]. Therefore, we initiated the study by testing two different incubation periods, using previously described dopamine concentration (Section 4.2-2.1). OCA measurements revealed that, independently of the incubation periods tested (18 h and 24 h), a significant wettability increase was observed after pDA incubation, which is in accordance to the previously reported studies [99], [100], [101]. Additionally, XPS analysis revealed an increased in the relative percentage of N that is in agreement with amino containing groups (NH_2) reported when

introducing pDA layers [102]. The polymerization of pDA on PU surfaces was also supported by the observation of a smooth topographical feature in SEM analysis.

Plasma surface modifications were performed to take advantage from the introduced functional groups at the surface that could improve coating linkage to substrate. Depending on the type of gas used, power applied and duration of plasma, it is possible to change the hydrophilicity of the surface independently of the bulk structure [96], [103]. Here two different reactive gases (O_2 or N_2) were tested using a high-density atmospheric plasma. Generally, O_2-plasma treatment leads to the introduction of oxygen-containing functional groups, such as carboxylic acid, peroxide (due to post-plasma reactions) and hydroxyl groups. Nitrogen, ammonia and N_2/H_2-plasmas usually introduce nitrogen-containing groups [36], [37]. Atomic composition of plasma treated surfaces using both gases expressed a slight decrease of C/O ratio when compared to PU suggesting that an alteration of PU surface atomic composition was actually taken place. Surprisingly, N_2-plasma and O_2-plasma treatments introduced similar atomic composition, having an increase in O contribution while maintaining the levels of N. In fact, previous studies have reported the same type of atomic composition alteration [104]. Atmospheric N_2-plasma-treated samples can react with atmospheric air that induce a post-plasma functionalization. In this sense, it is possible to consider that functionalization with nitrogen plasma was obtained by insertion of oxygen-containing species as a consequence of the post-plasma functionalization derived from exposure to atmospheric air [35]. This explanation can be sustained by contact angle results, where a similar wettability increase was observed on plasma-treated surfaces using both O_2 and N_2 gases, particularly when using medium/high intensity P2/P3 plasma parameters combination. This similarity in wettability suggests that the efficiency of plasma surface activation was independent of the type of selected reactive gas. In order to reduce costs and the risk excessive discharges [105], P2 parameters combination was selected for further surface modifications and analysis, since we were applying less power. Nevertheless, if specific chemical introduction of N_2 containing groups were desired, it could be performed by introducing vacuum to the system. However, increasing demands from industry encourage the continuous development of more efficient and more flexible plasma techniques, such as the atmospheric pressure technology-based plasma reactors, which overcome the disadvantages of low pressure. Indeed atmospheric plasma technology can easily be scaled up to industrial dimensions and integrated on in-line processes, since the investment costs are much lower in comparison to the use of vacuum devices [32]. As performed here, several other authors have also reported the use of atmospheric plasma for the modification of surfaces of materials in a successful way [106], [107].

The stability of the plasma activation was verified by evaluating the aging of samples during 3 days after activation on dry environment (argon). Results revealed that surfaces have gone through an hydrophobic recovery where part of the generated effect was lost, which is in accordance to previous studies [38]. Indeed, the reorientation of the polar groups toward the interface could be an explanation for this phenomenon, as a surface has the tendency to minimize the interfacial energy. This was also observed on O_2-plasma-treated

polydimethylsiloxane (PDMS) surface that was aged in air, and with time the surface returned to a low-energy-state [129]. Taking in consideration this hydrophobic recovery, posterior RPS polymer deposition onto the activated PU was always performed a few hours after plasma pre-treatments in order to take advantage of highest rates of surface activation. Nevertheless, a preliminary assay regarding contact angle monitoring of plasma treated surfaces stored in type I water (instead of argon) have shown that the surface hydrophobic recovery was not so pronounced, exhibiting a longer effect of surface activation (supplementary material and data, fig. S1). This observation is in good agreement with previous studies [108] and may be related to the minimization of the interfacial free energy by the water, by expanding the polar groups toward the polar solvent.

Regarding ozone pre-treatment, ozone exposure is known to promote surface oxidation through the introduction of highly reactive gas species (atomic oxygen and ozone molecules) that may react with the surfaces of polymers to form moieties (peroxy and hydroxyl radicals, hydroperoxide, carbonyl, and carboxyl [109]), which are responsible for the increased adhesion of added compounds to the polymer surfaces [42]. The number of these radicals and functional groups produced during the treatment are dependent on the ozone concentration and the exposure time [109]. Polymer degradation caused by the ozone attack must also be taken into account, since previous studies have shown the deterioration of PU when exposed to prolonged (hours) ozone treatment [41]. However, additionally to the results presented here, other studies have suggested that when using short periods of ozone exposure (minutes), it is also possible to efficiently activate polymer surfaces without affecting the bulk structure [110] and with reduced rates of polymer degradation. Here, an adapted and simple ozone surface treatment methodology was used, which resulted on altered PU surface topography and improved surface hydrophilicity that is in accordance with studies reporting ozone treated polyurethane surfaces [109]. Surprisingly, obtained atomic composition regarding activated surfaces through this technique, expressed lower amounts of oxygen and higher rates of carbon in comparison to unmodified PU surfaces, a fact that is not in accordance with previously reported introduction of oxygen-containing species characteristic for this kind of treatment [109]. Nevertheless, since this type of activation was detected by OCA and SEM, we hypothesise that this particular sample was not successfully and fully activated, probably due to operational problems on ozone generator at the time of sample preparation for XPS analysis.

Similarly to plasma surface treatments, reorientation at the surface after ozone activation also seemed to occur [111]. In fact, other studies have also shown the hydrophobic recovery of ozone treated surfaces [111], [43]. As a consequence, and similarly to plasma-treated surfaces, subsequent RPS polymer deposition onto the activated PU was always performed a few hours after ozone pre-treatments in order to take advantage of highest rates of surface activation.

Along with the tested surface pre-treatments, two different types of coating application methods were tested (immersion- and spin-coating). OCA results revealed a more pronounced wettability increase when applying RPS by spin-coating, independently of the pre-

treatment applied to PU, suggesting that, contrary to immersion-coating, this technique was effective for RPS coating application. Therefore, spin-coating was selected for further coating characterization and performance evaluation.

XPS analysis of the different coated surfaces presented the major elements previously reported to constitute *Cyanothece* RPS, which included C and O (characteristic of the polysaccharide nature of the polymer) [68]. In this study, although the C/O ratio was superior to previously reported RPS composition (C/O ratio of 1 [68]), in general all coatings expressed an increase of O element that suggests the presence of RPS coating on top of pre-treated PU surfaces. Moreover, other elements with less representation that have also been reported to constitute RPS (S from sulphate groups (10% of polymer composition) and N from existing peptides not covalently linked to RPS [68]) also appeared on the atomic composition of coated surfaces, although with some differences depending on the coating production strategy. Given the low representation of S element and the possibility of N-containing peptides be easily removed from RPS, the non-detection of these elements was expected when analysing different coated samples. Additionally, plasma and ozone strategies have shown a less pronounced decrease of C/O ratios in comparison to pDA strategy. This may suggest that the pDA linkage was capable of producing more uniform and thicker RPS coatings on top of PU surfaces, being easily detected by XPS (that only analyse the upper top fraction of the surface). The industrial-like activation processes introduced the modifications at the superficial layer of PU, which influenced the final coating thickness (thinner than pDA layer application), and the overall XPS detection of plasma and ozone pre-treatments as well as consequent coatings deposition. Nevertheless, Alcian Blue staining of the different produced coatings revealed the successful deposition and linkage of RPS polymer to the PU surface, independently of the pre-activation treatment.

Regarding the susceptibility of the coated surfaces to different pH and temperature tested, the evaluation was performed by looking for an increase in contact angle values after the exposure to these conditions, which would be an indication of possible coating degradation. Generally, all types of produced coatings presented none or reduced rates of coating degradation since there was not a significant decrease on wettability of coatings exposed to the accelerated degradation conditions.

Finally, coatings were evaluated regarding its bacteria adhesion prevention potential against clinically relevant Gram-positive (*S. aureus*, *S. epidermidis)* and Gram-negative (*E. coli)* bacteria [112]. In the absence of plasma proteins, coatings produced through pDA strategy have strongly prevented bacterial adhesion, achieving >93% *S. aureus, S. epidermidis* and *E. coli* adhesion reduction rates when compared to uncoated PU. On the other hand, coatings produced through the industrial-like surface activation processes have also expressed a strong prevention on bacterial adhesion. Ozone strategy was able to prevent bacterial adhesion up to 99% using both tested bacteria whereas coatings produced through O_2 and N_2-plasma have reduced *S. aureus* adhesion up to 93%. However, it should be considered that when using *E. coli* as a bacterial model, coatings produced through plasma strategy appeared to have a less

pronounced effect on bacterial adhesion (73% reduction rate). Moreover, challenging the produced coatings with bacteria in the presence of human plasma proteins have shown to influence *S. aureus* and *S. epidermidis* adhesion in distinct ways. Contrary to *S. epidermidis*, where the absence or presence of blood plasma have not influenced bacterial attachment, *S. aureus* adhesion appeared to be enhanced in the presence of plasma proteins. It is well known that when a biomaterial is implanted in contact with blood, plasma proteins can rapidly adsorb onto the material surface to form a "conditioning film". This adsorbed protein layer may minimize the effect of biomaterial surface properties on bacterial adhesion [113]. *In vitro* studies have shown that the presence or absence of plasma proteins is not necessarily so straightforward. Plasma proteins have shown to influence bacterial adhesion in different manners, depending on the type of bacteria and protein concentrations. [114], [115], [116], [117], [118]. The increase in bacteria adhesion related to adsorbed plasma proteins is due to specific ligand/receptor events between plasma proteins and bacterial cell surface proteins known as the microbial surface components recognizing adhesive matrix molecules (MSCRAMM) [119]. Therefore here, the differences on bacterial ligands/receptors may actually explain these differences in the presence or absence of plasma using different bacteria. Additional studies regarding the interactions between surface, plasma proteins and bacteria, would result in a deeper knowledge regarding the real potential of produced RPS coatings [120]. In the anti-adhesive assays using *E. coli*, plasma proteins were not used since this pathogen is mostly found in urological mucosa where blood plasma is not an issue [121].

The data herein reported strongly suggests the overall efficiency of the selected strategies on coating production, as well as the real potential of this particular polymer application as anti-adhesive coatings using PU as substrate. Actually, the bacterial reduction rates reported here are more dramatic than other reported polysaccharide-based coatings [53], [52], [122], [123]. Coating anti-adhesive performance is usually a result from the superficial physical-chemical interactions between bacterial cell and coated surfaces. Here, RPS-coating is less prone to bacterial adhesion possibly due to its hydrophilic character, demonstrated by the expression of low water contact angles, independently of the coating production strategy. Moreover, since bacterial cell wall or membrane are negatively charged, the anionic character of RPS due to its composition (presence of two different uronic acids and sulphate groups) may also contribute to electrostatic repulsion of bacteria [124]. Another mechanism that can possibly explain RPS coating anti-adhesive performance is the creation of a steric barrier that is highly related with improved wettability and surface hydration. The density of the polymeric chains can provide a steric barrier that repels bacterial adhesion by minimizing covalent interactions [24].

Besides the overall coating production strategies evaluation on RPS deposition and linkage to PU, other factors should be taken into consideration when considering overall coating development, such as the scalability and cost-effectiveness of the adopted processes. Since the pDA linkage is difficult to translate to an industrial setting, the other types of industrial-like methodologies, plasma and ozone activations, can be considered to be more adequate for

this purpose [41], [96]. Operational costs regarding both processes should not be neglected since it is desired the most efficient RPS coating production and establishment with the lowest required expenditures. In fact, although it is possible to modify biomaterial surfaces without using hazardous solvents and affecting bulk properties using both processes, there are some differences that should be emphasised. The atmospheric plasma system used here requires less than a second for the activation of surfaces, while ozone process takes several minutes. Therefore, in terms of time, plasma strategy arises as the best option. Nevertheless, the fact that plasma is a more intensive treatment requiring high energetic levels for the introduction of reactive species with the use of two different gases (Air and O_2 or N_2), brings the costs of both processes to a similar level. On the other hand, when considering the treatment of complex shaped materials like catheters, ozonisation process could have an advantage since the bioreactor atmosphere is fully saturated with ozone, making possible the treatment of the entire materials, independently of its shape complexity.

Chapter 7

Conclusions and future perspectives

The aim of the current work was to develop an anti-adhesive coating based on released polysaccharides (RPS) from a cyanobacterial strain, *Cyanothece* sp. CCY 0110, in order to reduce bacterial adhesion and consequently prevent biofilm formation on indwelling devices, such as polyurethane catheters.

During the first part, a 5-fold scale-up of *Cyanothece* sp. CCY 0110 culture was established using 5 L bioreactors, which did not negatively affect *Cyanothece* growth and carbohydrates production. A good amount of isolated and purified polymer was obtained. However, it is still necessary to perform some optimization procedures of the culture conditions (light intensity, aeration and/or stirring) to improve further the growth rate. Moreover, the search for optimized methods and conditions able to improve polymer production and its isolation/purification will allow to achieve the most cost-effective yields, a factor extremely important for consequent industrial application, namely as a coating.

Additionally, the reduction of media cost without compromising *Cyanothece* growth and carbohydrates production is also extremely important. Results regarding the two different reduced cost media that were tested (ASNIII with sea water and NutriBloom Plus with sea water) suggested the possibility of reducing media costs without negatively affecting the sustainable growth and carbohydrates production of *Cyanothece*.

Regarding to the second part of the work (coating development), through different surface characterization techniques (optical contact angle, scanning electron microscopy, x-ray photoelectron microscopy and Alcian blue staining of RPS coated surfaces) it was possible to observe the potential of coating production via pDA, O_2/N_2-plasma and ozone strategies for the overall efficient linkage of RPS polymer to PU surface. Nevertheless, some differences were observed on the obtained coating deposition densities that should be further investigated and optimized, particularly when using O_2/N_2-plasma and ozone treatments.

Most of the produced coatings exhibited a good resistance to accelerated degradation conditions exhibiting none or reduced rates of coating degradation. Moreover, they revealed a strongly improved bacterial anti-adhesive performance in comparison to PU. Coatings produced via pDA layer strategy appeared to greatly reduce the adhesion of a broad-spectrum of bacteria, either in the absence or presence of blood plasma achieving >93% *S. aureus, S. epidermidis* and *E. coli* adhesion reduction rates when compared to uncoated PU. Nevertheless, contrary to *S. epidermidis*, *S. aureus* adhesion appeared to be influenced by the presence of plasma proteins where a less pronounced effect of the RPS-coating on adhesion reduction rates was observed. On the other hand, coatings produced through the industrial-like processes have also expressed a strong influence on bacterial adhesion in the absence of blood plasma. Ozone strategy was able to prevent bacterial adhesion up to 99% using both tested bacteria whereas coatings produced through O_2/N_2-plasma strategy have reduced *S. aureus* adhesion up to 93%. Nevertheless, results regarding *E. coli* adherence to coatings produced through plasma strategy, suggest that is necessary to further optimize of the overall process. Moreover, additional evaluations regarding other types of bacteria, as well as the interactions with plasma proteins, should be of interest. Furthermore, optimization of immersion-coating procedure should also be considered, as well as the possibly of exploring other types of coating deposition procedures, more adjusted for an industrial application (electro-spraying technique for example [125]), in order to achieve the highest rates of cost-effectiveness on RPS coating production.

Supplementary data

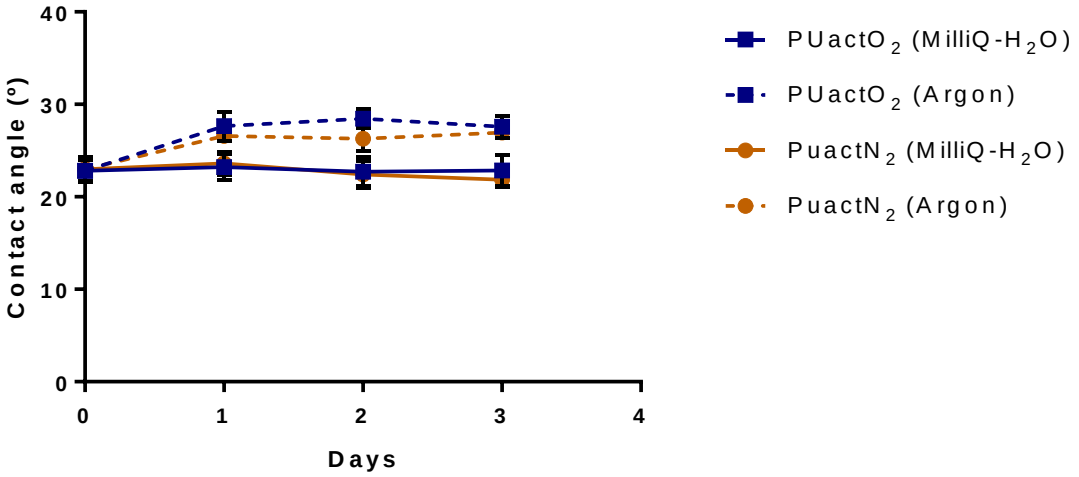

Fig. S1 - OCA captive bubble measurements (Tangent fitting method) of O_2/N_2 plasma treated surfaces ($PUactO_2/N_2$) throughout 3 days. The values are means ± standard deviations (n = 3, 1 assay).

Bibliography

[1] B. J. C. von Eiff, W. Kohnen, and K. Becker, "Modern strategies in the prevention of implant-associated infections", *International Journal of Artificial Organs*, vol. 28, pp. 1146-1156, 2005.

[2] S. S. Magill, J. R. Edwards, W. Bamberg, Z. G. Beldavs, G. Dumyati, M. A. Kainer, R. Lynfield, M. Maloney, L. McAllister-Hollod, J. Nadle, S. M. Ray, D. L. Thompson, "Multistate Point-Prevalence Survey of Health Care – Associated Infections", *New England Journal of Medicine*, vol. 370, pp. 1198–1208, 2014.

[3] C. von Eiff, B. Jansen, W. Kohnen, and K. Becker, "Infections Associated with Medical Devices", *Drugs*, vol. 65, pp. 179-214, 2005.

[4] K. S. Huang, C. H. Yang, S. L. Huang, C. Y. Chen, Y. Y. Lu, and Y. S. Lin, "Recent advances in antimicrobial polymers: A mini-review", *International Journal of Molecular Sciences*, vol. 17, pii: E1578, 2016.

[5] B. W. Trautner and R. O. Darouiche, "Catheter associated infections", *JAMA Internal Medicine*, vol. 164, pp. 842-850, 2004.

[6] P. Vergidis and R. Patel, "Novel Approaches to the Diagnosis, Prevention and Treatment of Medical Device-Associated Infections," *Infectious Disease Clinics of North America*, vol. 26, no. 1, pp. 173–186, 2013.

[7] I. Francolini, G. Donelli, F. Crisante, and V. Taresco, "Biofilm-based Healthcare-associated Infections", *Advances in Experimental Medicine and Biology*, vol.830, pp. 93-117, 2015.

[8] Z. K. Zander and M. L. Becker, "Antimicrobial and Antifouling Strategies for Polymeric Medical Devices", *ACS Macro Letters*, vol. 24, pp. 6484-6489, 2018.

[9] G. S. Lorite, C. M. Rodrigues, A. A. De Souza, C. Kranz, B. Mizaikoff, and M. A. Cotta, "The role of conditioning film formation and surface chemical changes on Xylella fastidiosa adhesion and biofilm evolution" *Journal of Colloid Interface Sciences*, vol.359, pp. 289-295, 2011.

[10] P. Watnick and R. Kolter, "Biofilm, City of Microbes", *Journal of Bacteriology*, vol. 182, pp. 2675–2679, 2000.

[11] J. W. Costerton, "Bacterial Biofilms: A Common Cause of Persistent Infections", *Science*, vol. 284, pp. 1318-22, 1999.

[12] E. M. Hetrick and M. H. Schoenfisch, "Reducing implant-related infections: active release strategies," *Chemical Society. Reviews*, vol. 35, pp. 780-789, 2006.

[13] H. Shah, W. Bosch, K. M. Thompson, and W. C. Hellinger, "Intravascular Catheter-Related Bloodstream Infection", *The Neurohospitalist,* vol. 3, pp. 144-151, 2013.

[14] T. M. Hooton, S. F. Bradley, D. D. Cardenas, R. Colgan, S. E. Geerlings, J. C. Rice, S. Saint, A. J. Schaeffer, P. A. Tambayh, P. Tenke, and L. E. Nicolle, "Diagnosis, Prevention, and Treatment of Catheter- Associated Urinary Tract Infection in Adults: 2009 International Clinical Practice Guidelines from the Infectious Diseases Society of America", *Clinical Infectious Diseases*, vol. 50, pp. 6625-663, 2010.

[15] L. E. Nicolle, "Urinary Catheter-Associated Infections", *Infectous Disease Clinics of North America*, vol. 26, pp. 13-27,2012.

[16] L. E. Nicolle, "Catheter associated urinary tract infections", *Antimicrobial Resistance & Infection Control*, vol. 3, pp. 1-8, 2014.

[17] L. Arnoldo, R. Migliavacca, L. Regattin, A. Raglio, L. Pagani, E. Nucleo, M. Spalla, F. Vailati, A. Agodi, A. Mosca, C. Zotti, S. Tardivo, I. Bianco, A. Rulli, P. Gualdi, P. Panetta, C. Pasini, M. Pedroni and S. Brusaferro, "Prevalence of urinary colonization by extended spectrum-beta-lactamase Enterobacteriaceae among catheterised inpatients in Italian long term care facilities", *BMC Infectious Diseases*, vol. 13, pp. 124-?, 2013.

[18] M. Kołpa, M. Wałaszek, A. Gniadek, Z. Wolak, and W. Dobroś, "Incidence, Microbiological Profile and Risk Factors of Healthcare-Associated Infections in Intensive Care Units: A 10 Year Observation in a Provincial Hospital in Southern Poland", *International Journal of Environmental Research and Public Health*, vol. 84, pp. 1-16, 2018.

[19] S. R. Shah, A. M. Tatara, R. N. D. Souza, A. G. Mikos, and F. K. Kasper, "Evolving strategies for preventing biofilm on implantable materials", *Materials Today*, vol. 16, pp. 177-182, 2013.

[20] C. Desrousseaux, V. Sautou, S. Descamps, and O. Traoré, "Modification of the surfaces of medical devices to prevent microbial adhesion and biofilm formation," *Journal of Hospital Infections*, vol. 85, pp. 87-93, 2013.

[21] F. Siedenbiedel and J. C. Tiller, "Antimicrobial polymers in solution and on surfaces: Overview and functional principles," *Polymers*, vol. 4, pp. 46-71, 2012.

[22] L. Xu and C. A. Siedlecki, "*Staphylococcus epidermidis* adhesion on hydrophobic and hydrophilic textured biomaterial surfaces", *Biomedical Materials*, vol. 9, 2014.

[23] D. Perera-Costa and J. M. Bruque, "Studying the Influence of Surface Topography on Bacterial Adhesion using Spatially Organized Microtopographic Surface Patterns", *Langmuir*, vol. 30, pp. 4633–4641, 2014.

[24] S. Chen, L. Li, C. Zhao, and J. Zheng, "Surface hydration: Principles and applications toward low-fouling / nonfouling biomaterials", *Polymer*, vol. 51, pp. 5283-5293, 2010.

[25] G. Cheng, Z. Zhang, S. Chen, J. D. Bryers, and S. Jiang, "Inhibition of bacterial adhesion and biofilm formation on zwitterionic surfaces," *Biomaterials*, vol. 28, pp. 4192–4199, 2007.

[26] D. Campoccia, L. Montanaro, and C. Renata, "Biomaterials A review of the biomaterials technologies for infection-resistant surfaces", *Biomaterials*, vol. 34, pp. 8533-8554, 2013.

[27] X. Zhou, T. Zhang, X. Jiang, and N. Gu, "The Surface Modification of Medical Polyurethane to Improve the Hydrophilicity and Lubricity: The Effect of Pretreatment", *Journal ofApplied Polymer Science*, vol. 116, pp. 1284-1290, 2009.

[28] M. Li, "Surface modification strategies for combating catheter-related complications : recent advances and challenges", *Journal of Matererials Chemistry*, vol. 5, pp. 2045-2067, 2017.

[29] A. M. F. Desimone, "Antimicrobial activity on glass materials subject to disinfectant xerogel coating", *Journal of Industrial Microbiology and Biotechnology*, vol. 33, pp. 343–348, 2006.

[30] J. Li, S. Zivanovic, P. M. Davidson, and K. Kit, "Production and characterization of thick, thin and ultra-thin chitosan / PEO films", *Carbohydrate Polymers*, vol. 83, pp. 375-382, 2011.

[31] W. Tillmann and E. Vogli, "Selecting Surface-treatment Technologies", *Modern Surface Technology*, pp. 1-10, 2006.

[32] T. Desmet, R. Morent, N. De Geyter, C. Leys, E. Schacht, and P. Dubruel, "Nonthermal Plasma Technology as a Versatile Strategy for Polymeric Biomaterials Surface Modification: A Review", *Biomacromolecules*, vol. 10, pp. 2351-2378, 2009.

[33] H. Lee, S. M. Dellatore, W. M. Miller, and P. B. Messersmith, "Mussel-Inspired Surface

Chemistry for Multifunctional Coatings", *Science*, vol. 318, pp. 426-430, 2008.

[34] C. H. Kwong, S. P. Ng, C. W. Kan, and R. Molina, "Inducing Hydrophobic Surface on Polyurethane Synthetic Leather by Atmospheric Pressure Plasma", *Fibers and Polymers*, vol. 15, pp. 1596-1600, 2014.

[35] M. R. Sanchis, O. Calvo, O. Fenollar, D. Garcia, and R. Balart, "Surface Modification of a Polyurethane Film by Low Pressure Glow Discharge Oxygen Plasma Treatment", *Journal of Applied Polymer Science*, vol. 105, pp. 1077-1085, 2007.

[36] Z. Wang, L. Wan, and Z. Xu, "Surface engineerings of polyacrylonitrile-based asymmetric membranes towards biomedical applications: An overview", *Journal of Membrane Science*, vol. 304, pp. 8-23, 2007.

[37] Y. Zhu, C. Gao, X. Liu, and J. Shen, "Surface Modification of Polycaprolactone Membrane via Aminolysis and Biomacromolecule Immobilization for Promoting Cytocompatibility of Human Endothelial Cells", *Biomacromolecules*, vol. 3, pp. 1312–1319, 2002.

[38] T. Jacobs, R. Morent, N. De Geyter, P. Dubruel, and C. Leys, "Plasma Surface Modification of Biomedical Polymers: Influence on Cell-Material Interaction", *Plasma Chemistry and Plasma Processing*, vol. 32, pp. 1039–1073, 2012.

[39] W. Yan, Z. J. Han, W. Z. Liu, X. P. Lu, B. T. Phung and K. Ostrikov, "Designing Atmospheric-Pressure Plasma Sources for Surface Engineering of Nanomaterials", *Plasma Chemistry and Plasma Processing*, vol. 33, pp. 479–490, 2013.

[40] G. Xu, Y. Ma and G. Zhang, "DBD Plasma Jet in Atmospheric Pressure Argon", *IEEE Transactions On Plasma Science*, vol. 36, pp. 1352-1353, 2016.

[41] K. Fujimoto and Y. Ikada, "Ozone-Induced Graft Polymerization onto Polymer Surface", *Journal of Polymer Science*, vol. 31, pp. 1035-1043, 1993.

[42] L. P. Haack, A. M. Straccia, J. W. Holubka, A. Bhurke, M. Xie, and L. T. Drzal, "Chemistry of surface modification with UV / ozone for improved intercoat adhesion in multilayered coating systems", *Surface Interface and Anal*ysis, vol. 836, pp. 829-836, 2000.

[43] H. Hillborg and G. J. Vancso, "Hydrophobic recovery of UV / ozone treated poly (dimethylsiloxane): adhesion studies by contact mechanics and mechanism of surface modification", *Applied Surface Science*, vol. 239, pp. 410-423, 2005.

[44] C. Zhang, L. Gong, L. Xiang, Y. Du, W. Hu, H. Zeng and Z. K. Hu, "Deposition and Adhesion of Polydopamine on Surfaces of Varying Wettability", *Applied Materials Interfaces,* vol. 9, pp. 30943–30950, 2017.

[45] S. H. Yang, S. M. Kang, K. Lee, T. D. Chung, H. Lee, and I. S. Choi, "Mussel-Inspired Encapsulation and Functionalization of Individual Yeast Cells", *Journal of the American Chemical Society*, vol. 133, pp. 2795–2797, 2011.

[46] H. C. Terrill, "Optimization of Polydopamine Coatings", *Honors Research Projects*, vol. 84, 2015.

[47] W. Senaratne, L. Andruzzi, and C. K. Ober, "Self-Assembled Monolayers and Polymer Brushes in Biotechnology: Current Applications and Future Perspectives", *Biomacromolecules*, vol. 6, pp. 2427–2448, 2005.

[48] V. B. Damodaran and N. S. Murthy, "Bio-inspired strategies for designing antifouling biomaterials", *Biomaterials Research*, vol. 20, 2016.

[49] S. Bhatia, "Natural polymer drug delivery systems: Nanoparticles, plants, and algae", *Springer International Publishing Switzerland*, 2016.

[50] G. A. Junter, P. Thébault and L. Lebrun, "Polysaccharide-based antibiofilm surfaces Acta Biomaterialia Polysaccharide-based antibiofilm surfaces", *Acta Biomaterialia*, vol. 30, pp. 13-25, 2016.

[51] J. M. Goddard and J. H. Ã. Hotchkiss, “Polymer surface modification for the attachment of bioactive compounds”, *Progress in Polymer Sci*ence, vol. 32, pp. 698-725, 2007.

[52] Z. Shi, D. Ph, K. G. Neoh, D. Sc, E. Kang, and D. Ph, “Titanium with Surface-Grafted Dextran and Immobilized Bone Morphogenetic Protein-2 for Inhibition of Bacterial Adhesion and Enhancement of Osteoblast Functions”, *Tissue Engineering*, vol. 15, pp. 417-426, 2009.

[53] V. Gadenne, L. Lebrun, T. Jouenne, and P. Thébault, “Antiadhesive activity of ulvan polysaccharides covalently immobilized onto titanium surface”, *Colloids and Surfaces B: Biointerfaces*, vol. 112, pp. 229-236, 2013.

[54] B. A. Whitton and M. Potts, "Introduction to the Cyanobacteria", *In* B. A. Whitton, M. Potts (ed), The ecology of cyanobacteria: their diversity in time and space. Springer, Netherlands, pp. 1-11, 2000.

[55] P. Fay, “Oxygen Relations of Nitrogen Fixation in Cyanobacteria", *Microbiological Reviews*, vol. 56, pp. 340-373, 1992.

[56] T. Encarnação, A. A. Pais, M. G. Campos and H. D. Burrows, “Cyanobacteria and microalgae: A renewable source of bioactive compounds and other chemicals”, *Science Progress*, vol. 98, pp. 145-68, 2016.

[57] S. Pereira, A. Zille, E. Micheletti, P. Moradas-ferreira, R. De Philippis, and P. Tamagnini, “Complexityof cyanobacterial exopolysaccharides: composition, structures, inducing factors and putative genes involved in their biosynthesis and assembly”, *FEMS Microbiology Reviews*, vol. 33, pp. 917-941, 2009.

[58] A. Parikh and D. Madamwar, “Partial characterization of extracellular polysaccharides from cyanobacteria”, *Bioresource Technology*, vol. 97, pp. 1822-1827, 2006.

[59] R. D. E. Philippis, M. C. Margheri, R. Materassi, and T. Alimentari, “Potential of Unicellular Cyanobacteria from Saline Environments as Exopolysaccharide Producers”, *Applied And Environmental Microbiology*, vol. 64, pp. 1130-1132, 1998.

[60] B. Nicolaus, A. Panico, I. Romano, M. C. Manca, A. De Giulio, and A. Gambacorta, “Chemical composition and production of exopolysaccharides from representative members of heterocystous and non-heterocystous cyanobacteria”, *Phytochemistry*, vol. 52, pp. 639-647, 1999.

[61] R. De Philippis and M. Vincenzini, “Exocellular polysaccharides from cyanobacteria and their possible applications”, *FEMS Microbiology Reviews*, vol. 22, pp. 151-175, 1998.

[62] I. W. Sutherland, “Structure-function relationships in microbial exopolysaccharides”, *Biotechnology Advances*, vol. 12, pp. 393-448, 1994.

[63] S. Arias, A. del Moral, M. R. Ferrer, E. Quesada, and V. Béjar, “Mauran , an exopolysaccharide produced by the halophilic bacterium *Halomonas maura*, with a novel composition and interesting properties for biotechnology”, *Extremophiles*, vol. 7, pp. 319–326, 2003.

[64] A. Tabernero, E. M. Martín, and M. A. Galan, “Microalgae Technology: A Patent Survey”, *International Journal of Chemical Reactor Engineering*, vol. 11, 2013.

[65] Y. Hayakawa, “Calcium spirulan as an inducer of tissue-type plasminogen activator in human fetal lung fibroblasts”, *Biochimica et Biophysica Acta*, vol. 1355, pp. 241-247, 1997.

[66] J. Lee, X. Hou, K. Hayashi, and T. Hayashi, “Effect of partial desulfation and oversulfation of sodium spirulan on the potency of anti-herpetic activities”, *Carbohydrate Polymers*, vol. 69, pp. 651-658, 2007.

[67] E. Micheletti, G. Colica, C. Viti, P. Tamagnini, and R. De Philippis, “Selectivity in the heavy metal removal by exopolysaccharide-producing cyanobacteria”, *Journal of Applied Microbiology*, vol. 105, pp. 88-94, 2008.

[68] R. Mota, R. Guimarães, Z. Büttel, F. Rossi, G. Colica, C. J. Silva, L. Gales, A. Zille, R. De Philippis, S. B. Pereira, and P. Tamagnini, "Production and characterization of extracellular carbohydrate polymer from *Cyanothece* sp. CCY 0110", *Carbohydrate Polymers*, vol. 92 , pp. 1408–1415, 2013.

[69] R. Mota, S. B. Pereira, M. Meazzini, R. Fernandes, A. Santos, C. A. Evans, R. De Philippis, P. C. Wright, and P. Tamagnini, "Effects of heavy metals on *Cyanothece* sp. CCY 0110 growth, extracellular polymeric substances (EPS) production, ultrastructure and protein profiles", *Journal of Proteomics*, vol. 120, pp. 75-94, 2015.

[70] J. P. Leite, R. Mota, J. Durão, S. C. Neves, C. C. Barrias, P. Tamagnini, and L. Gales, "Cyanobacterium-Derived Extracellular Carbohydrate Polymer for the Controlled Delivery of Functional Proteins", *Macromolecular Biosci*ense, vol. 17, 1600206, 2017.

[71] A. W. Neumann and R. Good, "Techniques of Measuring Contact Angles", *Surface and Colloid Science*, pp. 31-91, 1979.

[72] K. Y Law and H. Zhao, "Contact Angle Measurements and Surface Characterization Techniques", *Surface Wetting. Springer, Cham,* pp. 7-34, 2016.

[73] F. J. M. Ruiz-Cabello and A. Marmur, "Comparison of Sessile Drop and Captive Bubble Methods on Rough Homogeneous Surfaces: A Numerical Study", *Langmuir*, vol. 27, pp. 9638–9643, 2011.

[74] W. Zhang, and B. Hallstrom, "Membrane Characterization Using the Contact Angle Technique I. Methodology of the Captive Bubble Technique", *Desalination*, vol. 79, pp. 1-12, 1990.

[75] R. F. Egerton, "Physical Principles of Electron Microscopy: An Introduction to TEM, SEM, and AEM", *Springer Science+Business Media, Inc.*, pp. 1-202, 2005.

[76] F. Liu, J. Wu, K. Chen, and D. Xue, "Morphology Study by Using Scanning Electron Microscopy", *In* A. Méndez-Vilas and J. Díaz (Ed), Microscopy: Science, Technology, Applications and Education, Formatex Research Center, Spain, pp. 1781-1792, 2010.

[77] D. Yang, A. Velamakanni, G. Bozoklu, S. Park, M. Stoller, R. D. Piner, S. Stankovich, I. Jung, D. A. Field, C. A. Ventrice Jr., and R. S. Ruoff, "Chemical analysis of graphene oxide films after heat and chemical treatments by X-ray photoelectron and Micro-Raman spectroscopy", *Carbon*, vol. 7, pp. 1-8, 2008.

[78] D. R. Miller, "The Use Of X-Ray Photoelectron Spectroscopy For The Analysis Of The Surface Of Biomaterials", *Journal of Macromolecular Science*, vol. 26, pp. 33-66, 2014.

[79] S. G. Kazarian, and K. L. A. Chan, "ATR-FTIR spectroscopic imaging: recent advances and applications to biological systems", *Analyst*, vol. 138, pp. 1940-1951, 2013.

[80] K. L. A. Chan and S. G. Kazarian, "Detection of trace materials with Fourier transform infrared spectroscopy using a multi-channel detector", *Analyst*, vol. 131, pp. 126-131, 2006.

[81] R. Y. Stanier, "Generic Assignments , Strain Histories and Properties of Pure Cultures of Cyanobacteria", *Journal of General Microbiology*, vol. 110, pp. 1-61, 2018.

[82] D. C. O. Thornton, E. M. Fejes, S. F. Dimarco, and K. M. Clancy, "Measurement of acid polysaccharides in marine and freshwater samples using alcian blue", *Limnology and Oceanography: Methods*, vol. 5, pp. 73-87, 2007.

[83] S. L. Anderson and L. E. E. Mcintosh, "Light-Activated Heterotrophic Growth of the Cyanobacterium *Synechocystis* sp. strain PCC 6803: a Blue-Light-Requiring Process", *Journal of Bacteriology*, vol. 173, pp. 2761-2767, 1991.

[84] D. Kushwaha, S. N. Upadhyay, and P. K. Mishra, "Growth of Cyanobacteria: Optimization for Increased Carbohydrate Content", *Applied Biochemistry and Biotechnology*, vol. 184, pp. 1247–1262, 2017.

[85] M. Dubois, K. A. Gilles, J. K. Hamilton, P. A. Rebers, and F. Smith, “Colorimetric Method for Determination of Sugars and Related Substances”, *Nature*, vol. 28, pp. 350-356, 1951.

[86] M. C. Martins, D. Wang, J. Ji, L. Feng, and M. A. Barbosa, “Albumin and fibrinogen adsorption on Cibacron blue F3G-A immobilised onto PU-PHEMA surfaces F3G-A immobilised onto PU-PHEMA”, *Journal of Biomaterials Sciences, Polymer Edition*, vol. 14, pp. 439-455, 2003

[87] S. Pereira, E. Micheletti, A. Zille, A. Santos, P. Moradas-Ferreira, P. Tamagnini, and R. De Philippis, “Using extracellular polymeric substances (EPS)-producing cyanobacteria for the bioremediation of heavy metals: do cations compete for the EPS functional groups and also accumulate inside the cell?", *Microbiology*, vol. 157, pp. 451-458, 2011.

[88] Y. U. Guoce, S. H. I. Dingji, C. A. I. Zhaoling, and C. Wei, “Growth and Physiological Features of Cyanobacterium *Anabaena* sp. strain PCC 7120 in a Glucose-Mixotrophic Culture”, *Chinese Journal of Chemical Engineering*, vol. 19, pp. 108-115, 2011.

[89] K. J. Reddy, B. W. Soper, J. Tang, and R. L. Bradley, “Phenotypic variation in exopolysaccharide production in the marine, aerobic nitrogen-fixing unicellular cyanobacterium *Cyanothece* sp.”, *World Journal of Microbiology & Biotechnology*, vol. 12, pp. 311-318, 1996.

[90] G. Pierre, C. Delattre, G. Pierre, C. Laroche, and P. Michaud, “Production , extraction and characterization of microalgal and cyanobacterial exopolysaccharides”, *Biotechnology Advances*, vol. 34, pp. 1159-1179, 2016.

[91] A. K. Patel, C. Laroche, A. Marcati, A. V. Ursu, S. Jubeau, L. Marchal, E. Petit, G. Djelveh, and P. Michaud, “Separation and fractionation of exopolysaccharides from Porphyridium cruentum”, *Bioresource Technolology*, vol. 145, pp. 345-350, 2013.

[92] C. González-fernández and M. Ballesteros, “Linking microalgae and cyanobacteria culture conditions and key-enzymes for carbohydrate accumulation”, *Biotechnology Advances*, vol. 30, pp. 1655-1661, 2012.

[93] F. Fadel and A. E. Kamil, “Production and nutritive value of *Spirulina platensis* in reduced cost media”, *Egyptian Journal of Aquatic Research*, vol. 38, pp. 51-57, 2012.

[94] R. Dineshkumar, R. Narendran, and P. Sampathkumar, “Cultivation of *Spirulina platensis* in different selective media”, *Indian Journal of Geo Marine Sciences*, vol. 45, pp. 1749-1754, 2016.

[95] E. M. Liston, L. Martinu, and M. R. Wertheimer, “Plasma surface modification of polymers for improved adhesion: a critical review”, *Journal of Adhesion Sciences and Technology*, vol. 7, pp. 37-41, 1993.

[96] P. Taylor and Y. Kusano, “Atmospheric Pressure Plasma Processing for Polymer Adhesion: A Review”, *The Journal of Adhesion*, vol. 90, pp. 37-41, 2014.

[97] J. Drelich and J. D. Miller, “A systematic comparison of sessile-drop and captive-bubble contact angle methods”, *Society of Mining Engineers of Aime*, 1995.

[98] Y. Yuan and T. R. Lee, "Contact Angle and Wetting Properties", S*urface Science Techniques*, vol. 51, pp. 3-34, 2013.

[99] H. Li, Y. Jia, X. Feng, and J. Li, “Facile fabrication of robust polydopamine microcapsules for insulin delivery”, *Journal of Colloid Interface Science*, vol. 487, pp. 12-19, 2017.

[100] C. Cheng, S. Li, W. Zhao, Q. Wei, S. Nie, and S. Sun, “The hydrodynamic permeability and surface property of polyethersulfone ultrafiltration membranes with mussel-inspired polydopamine coatings”, *Journal of Membrane Science*, vol. 417-418, pp. 228-236, 2012.

[101] Z. Xi, Y. Xu, L. Zhu, Y. Wang, and B. Zhu, “A facile method of surface modification for

hydrophobic polymer membranes based on the adhesive behavior of poly (DOPA) and poly (dopamine)", *Journal of Membrane Science*, vol. 327, pp. 244-253, 2009.

[102] M. Vaselbehagh, H. Karkhanechi, S. Mulyati, R. Takagi, and H. Matsuyama, "Improved antifouling of anion-exchange membrane by polydopamine coating in electrodialysis process", *Desalination*, vol. 332, pp. 126-133, 2014.

[103] P. K. Chu, J. Y. Chen, L. P. Wang, and N. Huang, "Plasma-surface modification of biomaterials", *Materials Science and Engineering*, vol. 36, pp. 143-206, 2002.

[104] M. R. Sanchis, O. Calvo, O. Fenollar, D. Garcia, and R. Balart, "Characterization of the surface changes and the aging effects of low-pressure nitrogen plasma treatment in a polyurethane film", *Polymer Testing*, vol. 27, pp. 75-83, 2008.

[105] A. Fahmy and J. Friedrich, "Degradation behavior of thin polystyrene films on exposure to Ar plasma and its emitted radiation", *Journal of Adhesion Science and Technology*, vol. 27, pp. 324-338, 2012.

[106] F. Mwale, M. Iordanova, C. Demers, P. Desjardins, and M. R. Wertheimer, "Atmospheric Pressure Deposition of Micropatterned Nitrogen-Rich Plasma-Polymer Films for Tissue Engineering", *Plasma Processes and Polymers*, vol. 2, pp. 263-270, 2005.

[107] G. T. Lewis, G. R. Nowling, R. F. Hicks, and Y. Cohen, "Inorganic Surface Nanostructuring by Atmospheric Pressure Plasma-Induced Graft Polymerization", *Langmuir*, vol. 23, pp. 10756–10764, 2007.

[108] P. Alves, R. Cardoso, T. R. Correia, B. P. Antunes, I. J. Correia, and P. Ferreira, "Surface Modification of Polyurethane Films by Plasma and Ultraviolet Light to Improve Haemocompatibility for Artificial Heart Valves", *Colloids Surfaces B: Biointerfaces*, vol. 113, pp. 25-32, 2013.

[109] P. Kuang, J. Lee, C. Kim, K. Ho, and K. Constant, "Improved Surface Wettability of Polyurethane Films by Ultraviolet Ozone Treatment", *Journal of Applied Polymer Science,* vol. 118, pp. 3024-3033, 2010.

[110] M. J. Walzak, S. Flynn, R. Foerch, J. M. Hill, E. Karbashews, A. Lin and M. Strobel, "UV and ozone treatment of polypropylene and poly (ethylene terephthalate)", *Journal of Adhesion Science and Technology*, vol. 9, pp. 1229-1248, 2012.

[111] M. R. Davidson, S. A. Mitchell, and R. H. Bradley, "Surface studies of low molecular weight photolysis products from UV-ozone oxidised polystyrene", *Surface Science*, vol. 581, pp. 169-177, 2005.

[112] Barbara W. Trautner, and Rabih O. Darouiche, "Catheter-Associated Infections", *JAMA Internal Medicine*, vol. 164, pp. 842-850, 2004.

[113] K. Vacheethasanee, J. S. Temenoff, J. M. Higashi, A. Gary, J. M. Anderson, R. Bayston, and R. E. Marchant, "Bacterial surface properties of clinically isolated *Staphylococcus epidermidis* strains determine adhesion on polyethylene", *Journal of Biomedical Materials Research*, vol. 42, pp. 425-432, 1998.

[114] R. Ardehali, L. Shi, J. Janatova, S. F. Mohammad, and G. L. Burns, "The inhibitory activity of serum to prevent bacterial adhesion is mainly due to apo-transferrin", *Journal of Biomedical Materials Research*, vol. 66A, pp. 21-28, 2002.

[115] O. Hartford, L. O. Brien, K. Schofield, J. Wells, and T. J. Foster, "The Fbe (SdrG) protein of *Staphylococcus epidermidis* HB promotes bacterial adherence to fibrinogen", *Microbiology*, vol. 147, pp. 2545-2552, 2001.

[116] M. Hussain, C. Heilmann, G. Peters, and M. Herrmann, "Teichoic acid enhances adhesion of *Staphylococcus epidermidis* to immobilized fibronectin", *Microbial Pathogenesis*, vol. 32, pp. 261-270, 2001.

[117] W. M. Dunne and E. M. Burd, "Fibronectin and proteolytic fragments of fibronectin interfere with the adhesion of *Staphylococcus epidermidis* to plastic," *Journal of*

Applied Bacteriology, vol. 74, pp. 411-416, 1993.

[118] J. C. Linnes, K. Mikhova, and J. D. Bryers, "Adhesion of *Staphylococcus epidermidis* to biomaterials is inhibited by fibronectin and albumin", *Journal of Biomedical Materials Research*, vol. 100, pp. 1990–1997, 2012.

[119] L. Xu and C. A. Siedlecki, "Effects of Plasma Proteins on *Staphylococcus epidermidis* RP62A Adhesion and Interaction with Platelets on Polyurethane Biomaterial Surfaces", *Journal of Biomaterials and Nanobiotechnology*, vol. 3, pp. 487-498, 2012.

[120] B. Estevez and X. Du, "New Concepts and Mechanisms of Platelet Activation Signaling", *Physiology*, vol. 32, pp. 162-177, 2017.

[121] K. B. Laupland, D. B. Gregson, D. L. Church, T. Ross, and J. D. D. Pitout, "Incidence , risk factors and outcomes of *Escherichia coli* bloodstream infections in a large Canadian region", *Clinical Microbiology Infections*, vol. 14, pp. 10-16, 2008.

[122] M. F. Loke, S. Y. Lui, B. L. Ng, M. Gong, and B. Ho, "Antiadhesive property of microalgal polysaccharide extract on the binding of Helicobacter pylori to gastric mucin", *FEMS Immunology and Medical Microbiology*, vol. 50, pp. 231–238, 2007.

[123] P. Taylor, M. Morra, and C. Cassineli, "Non-fouling properties of polysaccharide-coated surfaces", *Journal of Biomaterials Science*, vol. 10, pp. 37-41, 2013.

[124] B. Gottenbos, D. W. Grijpma, H. C. Van Der Mei, J. Feijen, and H. J. Busscher, "Antimicrobial effects of positively charged surfaces on adhering Gram-positive and Gram-negative bacteria", *Journal of Antimicrobial Chemotherapy*, vol. 48, pp. 7-13, 2001.

[125] Q. Guo, J. P. Mather, P. Yang, M. Boden, and P. T. Mather, "Fabrication of Polymeric Coatings with Controlled Microtopographies Using an Electrospraying Technique", *PLOS ONE*, vol. 10, pp. 1-14, 2015.

[126] K. Gayad, C. Henry, and T. Owen, "http://www.google.com/patents/EP0891998A1?cl=en," 1999

[127] S. Chen and S. Jiang, "A New Avenue to Nonfouling Materials", *Advanced Materials*, vol. 20, pp. 335-338, 2007.

[128] H. P. Felgueiras, L. M. Wang, K. F. Ren, M. M. Querido, Q. Jin, M. A. Barbosa, J. Ji and M. C. L. Martins, "Octadecyl Chains Immobilized onto Hyaluronic Acid Coatings by Thiol−ene "Click Chemistry" Increase the Surface Antimicrobial Properties and Prevent Platelet Adhesion and Activation to Polyurethane", *ACS Applied Materials and Interfaces.*, vol. 9, pp. 7979–7989, 2017.

[129] H. Hillborg and G. J. Vancso, "Hydrophobic recovery of UV/ozone treated poly(dimethylsiloxane): adhesion studies by contact mechanics and mechanism of surface modification", *Applied Surface Science*, vol. 239, pp. 410-423, 2005.

[130] N. Lamba, K. Woodhouse, and S. Cooper, "Polyurethanes in biomedical applications", In *N.Hasirci, V. Hasirci (Ed), Biomaterials*, pp. 83-101, 1998.

[131] M. R. Davidson, S. A. Mitchell, and R. H. Bradley, "Surface studies of low molecular weight photolysis products from UV-ozone oxidised polystyrene", *Surface Science*, vol. 581, pp. 169-177, 2005.